Assessing population-level consequences of anthropogenic stressors for terrestrial wildlife

Todd E. Katzner [ID],[1,]† Melissa A. Braham [ID],[2] Tara J. Conkling [ID],[1] Jay E. Diffendorfer [ID],[3] Adam E. Duerr [ID],[4,5] Scott R. Loss [ID],[6] David M. Nelson [ID],[7] Hannah B. Vander Zanden [ID],[8] and Julie L. Yee [ID][9]

[1]*U.S. Geological Survey, Forest and Rangeland Ecosystem Science Center, Boise, Idaho, USA*
[2]*Division of Geology and Geography, West Virginia University, Morgantown, West Virginia, USA*
[3]*U.S. Geological Survey, Geosciences and Environmental Change Science Center, Denver, Colorado, USA*
[4]*Bloom Research, Los Angeles, California, USA*
[5]*Division of Forestry and Natural Resources, West Virginia University, Morgantown, West Virgini, USA*
[6]*Department of Natural Resource Ecology & Management, Oklahoma State University, Stillwater, Oklahoma, USA*
[7]*Appalachian Laboratory, University of Maryland Center for Environmental Science, Frostburg, Maryland, USA*
[8]*Department of Biology, University of Florida, Gainesville, Florida, USA*
[9]*U.S. Geological Survey, Western Ecological Research Center, Santa Cruz, California, USA*

Abstract.   Human activity influences wildlife. However, the ecological and conservation significances of these influences are difficult to predict and depend on their population-level consequences. This difficulty arises partly because of information gaps, and partly because the data on stressors are usually collected in a count-based manner (e.g., number of dead animals) that is difficult to translate into rate-based estimates important to infer population-level consequences (e.g., changes in mortality or population growth rates). However, ongoing methodological developments can provide information to make this transition. Here, we synthesize tools from multiple fields of study to propose an overarching, spatially explicit framework to assess population-level consequences of anthropogenic stressors on terrestrial wildlife. A key component of this process is using ecological information from affected animals to upscale from count-based field data on individuals to rate-based demographic inference. The five steps to this framework are (1) framing the problem to identify species, populations, and assessment parameters; (2) field-based measurement of the effect of the stressor on individuals; (3) characterizing the location and size of the populations of interest; (4) demographic modeling for those populations; and (5) assessing the significance of stressor-induced changes in demographic rates. The tools required for each of these steps are well developed, and some have been used in conjunction with each other, but the entire group has not previously been unified together as we do in this framework. We detail these steps and then illustrate their application for two species affected by different anthropogenic stressors. In our examples, we use stable hydrogen isotope data to infer a catchment area describing the geographic origins of affected individuals, as the basis to estimate population size for that area. These examples reveal unexpectedly greater potential risks from stressors for the more common and widely distributed species. This work illustrates key strengths of the framework but also important areas for subsequent theoretical and technical development to make it still more broadly applicable.

Key words: anthropogenic stressors; bats; birds; demographic impacts; integrated population model; renewable energy; stable isotope analysis.

† **E-mail:** tkatzner@usgs.gov

INTRODUCTION

Human activity influences wildlife. For example, on an annual basis in the United States, electric transmission and distribution lines kill between 12 and 64 million birds (Loss et al. 2014*a*), vehicle collisions kill between 89 and 340 million birds (Loss et al. 2014*b*), and wind turbines kill between 200,000 and 700,000 bats (Arnett and Baerwald 2013, Hayes 2013). However, the ecological and conservation significance of these fatalities is dependent on their population-level consequences, which in turn is influenced by factors like population size and life-history traits (e.g., reproductive strategy). As such, the human-caused death of 1 million *r*-selected chipping sparrows (*Spizella passerine*; U.S. population estimate 100 million; Partners in Flight (PIF) 2019) would be dramatically less relevant to population viability and conservation objectives than the death of 1% that number of deaths of *K*-selected golden eagles (*Aquila chrysaetos*; U.S. population estimate 40,000; PIF 2019). The demographic relevance of fatalities is also influenced by the size, demography, spatial distribution, and geographic origin of affected populations, as well as the timing of fatalities (Martin 2015, Griesser et al. 2017, Hunt et al. 2017). Furthermore, non-lethal anthropogenic stressors also can reduce offspring production or change behavior (Bonnington et al. 2013, Thompson et al. 2015, Winder et al. 2015) in ways that are consequential for populations.

These subtleties create challenges to understanding or predicting population-level responses of wildlife to lethal and non-lethal anthropogenic stressors. In fact, this process requires addressing a complex set of difficult-to-answer questions. These include (1) How many individuals have been affected? (2) How are those individuals affected (e.g., direct vs. indirect, lethal vs. sublethal, density-dependent vs. density-independent effects)? (3) How can the consequence of the stressor to those populations be characterized? (4) How large are the source populations for those individuals and how are they spatially organized? (5) How is it decided if those consequences are relevant?

The difficulty in answering these key questions comes in part because the information needed to solve them often is unavailable. However, ongoing methodological developments have resulted in new tools that can help provide that information. This methodological evolution comes on two fronts and at two spatial and demographic scales. One front is driven by the rapid expansion of renewable energy facilities and the creation of new regulations and guidelines to monitor site-specific impacts of these facilities on wildlife. The other arises from ecological or conservation-oriented fields of biogeographical study that consider data on a landscape or population scale.

At many renewable energy facilities, there have been environmental assessments to estimate pre-construction abundance of wildlife populations and post-construction numbers of fatalities (e.g., Conkling et al. 2020). These numerical assessments use a newly developed suite of field-based and statistical tools for collecting and interpreting survey data (e.g., Dalthorp et al. 2018). As a consequence, they often can answer the first key question above, about how many individuals are affected. That said, these environmental assessments are usually focused on numbers of individuals or fatalities at a single site, and they provide little information on larger-scale, population-level impacts (Loss et al. 2015).

Landscape- and population-scale tools developed in the last two decades provide a different set of information that could be useful to understanding how wildlife are affected by stressors (the second and third key question above). The study of migratory connectivity (Webster et al. 2002, Greenberg and Marra 2005, Cohen et al. 2018) characterizes linkages between geographically distinct areas used by a population during different portions of its annual cycle. Likewise, population viability analysis (PVA) is designed to inform conservation programs for at-risk species by assessing the relevance of stressors to population persistence (Morris et al. 1999). Finally, ecologically focused full annual cycle models evaluate the consequences of variation in demographic rates over different portions of organisms' annual cycles (e.g., breeding, migration, and stationary nonbreeding; Hostetler et al. 2015, Oberhauser et al. 2017, Rushing et al. 2017). All three of these tools are frequently applied at very broad spatial scales and can be effective at identifying how wildlife are affected.

However, with a few exceptions, they are not designed to incorporate individually based site-specific count data such as those described above.

Integration of these local- and landscape-scale tools is therefore an important priority, and it involves answering the fourth and fifth key questions above. Prior frameworks that have been proposed to combine these concepts generally address only a subset of those questions. As an example, published work has focused on defining the population of interest and the consequence of a stressor (Morrison and Pollock 1997), on defining if impact is consequential (Cook and Robinson 2017), and on the key considerations required for those two definitions (May et al. 2019). Likewise, prior efforts to integrate the identification of affected subpopulations with the estimation of population-level impacts generally have focused only on a single species (Pylant et al. 2016, Frick et al. 2017, Katzner et al. 2017) or a specific site (Smallwood and Thelander 2008, Desholm 2009) and thus are difficult to generalize across taxa, regions, and time periods.

As a result of this limited degree of integration, local count data are independent of the context provided by landscape-level information about the population of interest. Consequently, it can be difficult for conservation practitioners to interpret field-based count data in the context of population-level rates of change. In practical terms, this means that a site manager with counts of individuals killed can have difficulty interpreting the relevance of those data relative to reductions in the population growth rates. These difficulties inhibit assessments of the consequences to wildlife of many anthropogenic stressors (Loss et al. 2012, 2015). Making this leap, from count-based field data to rate-based estimates describing the larger population (i.e., upscaling; May et al. 2019), therefore is critical to interpreting the relevance of models describing the consequence of anthropogenic stressors on wildlife populations.

Here, we propose an overarching, spatially explicit approach to integrate site-specific and landscape- or population-scale tools into a single framework to assess population-level consequences of anthropogenic stressors. We begin by proposing a five-step framework to upscale from individual-level effects to population-level consequences. This process uses a series of well-developed tools from a variety of different fields, and, in each step, we provide background on these tools. Our proposed framework provides a novel, management-relevant unification of these separate tools. Next, we apply this framework to two specific cases for which we have data—solar energy caused fatalities of a range-restricted ground predator in the Mojave Desert, USA, and wind turbine caused fatalities of a widely distributed raptor species in central California, USA. Finally, we illustrate the broad applicability of our approach to other sources of anthropogenic fatality of wildlife, and we discuss gaps and next steps for further development of this analytical and conceptual framework.

Conceptual Framework

The five-step framework we propose to upscale from individual-level to population-level consequences integrates tools from the fields of ecology and conservation biology. The five steps in the framework (Fig. 1) are (1) framing the problem to identify species, populations, and assessment parameters; (2) using field-based count data to quantify the effect of the stressor on individuals; (3) characterizing the location and size of the population of interest; (4) building rate-based demographic models for the population; and (5) integrating information from steps 2, 3, and 4, to assess the significance to the population of the rate changes brought on by the stressor. These steps are detailed below.

Framing the problem

The first step in our proposed framework is planning and decision-making about the process itself, to identify key species, populations, and assessment parameters. Although it may seem too obvious to mention, this step bears discussion here because of the potential for a gap between research activity and implementation of conservation actions (Adams et al. 2019). When preparing to assess demographic effects to wildlife of anthropogenic stressors, it is therefore important that those implementing a research framework understand the goals and implementation capacity of key stakeholders. Key questions to address are the species on which to focus, how to define the population of interest (i.e., What population or
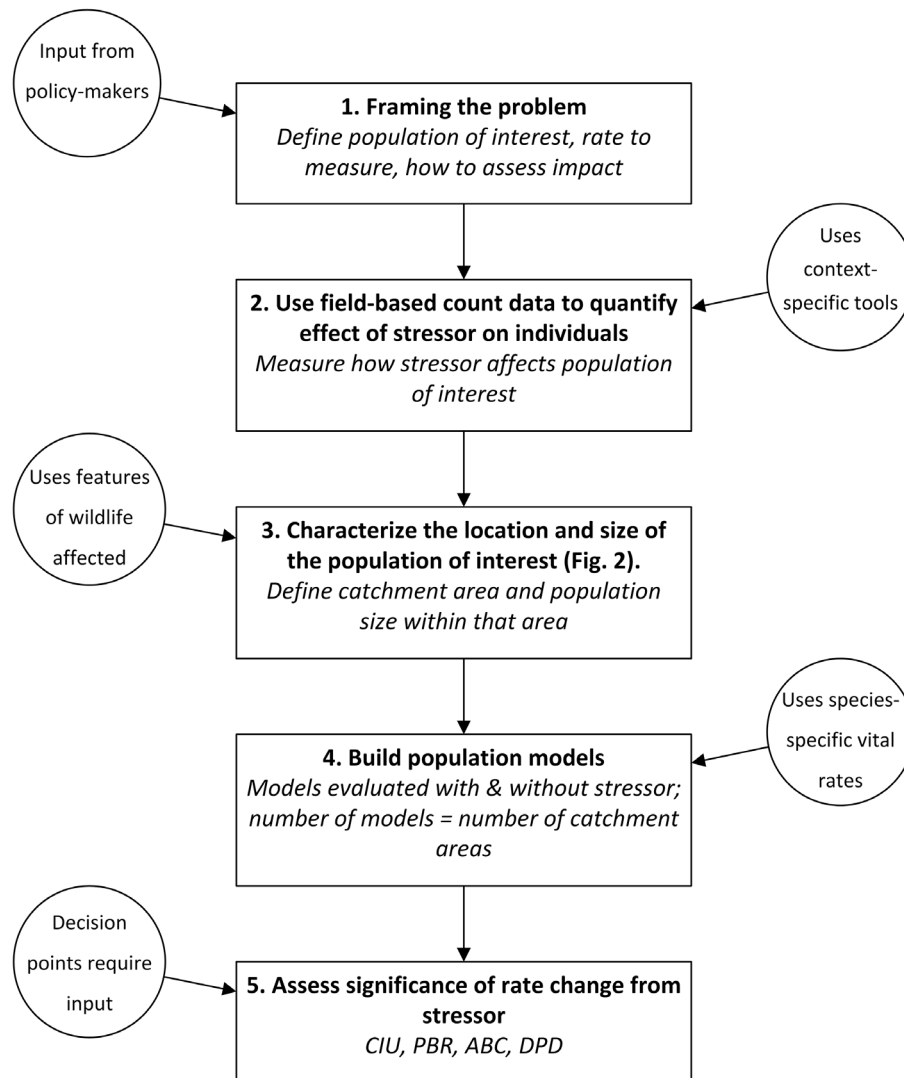
Fig. 1. Schematic of a proposed framework to assess population-level consequences of anthropogenic stressors on wildlife. Square boxes are steps in the process; circles are outside information required to process each step. Abbreviations in step 5 are described in the main text. Numbers for each step match those in Appendices S1, S2.

subpopulation is relevant to the stakeholders?), which demographic parameters should be the focus of comparisons (i.e., Are some parameters more or less likely to be affected by the stressor? Given local constraints, are some parameters more amenable to monitoring or potential mitigation?), what level or type of sampling is required to ensure sufficient statistical power to detect population change (Maclean et al. 2013, Sur et al. 2018), and how population-level effects will be evaluated (i.e.,

what are the costs and benefits of using the different types of assessment tools we outline in step 5 of the framework).

Use field-based count data to quantify the effect of the stressor on individuals

Once the initial framing of the problem is complete, the next step is to quantify stressor effects on individuals in the population of interest. To do this, context-specific data, usually field-based counts, need to be collected on the individuals

affected, and on the direction and magnitude of that effect. Such studies usually require an experimental design that allows comparison of monitoring data collected pre- and post-construction or on- and off-site (Conkling et al. 2020). In the case of direct mortality effects, design of field surveys requires estimation of detection and carcass removal rates (Huso 2011, Huso and Dalthorp 2014, Huso et al. 2016). Quantifying other parameters, including pre- and post-construction density or abundance, requires similar adjustments for detection probabilities (Bibby et al. 2000).

Characterize the location and size of the population of interest

The population of interest can be either the entire global population of a species or a subset of that population. Defining the size and location of the population of interest presents challenges and has implications for assessing population trends and demographic characteristics (Cook et al. 2011). This is especially the case when that definition incorporates spatial or temporal variation in location, age structure, or seasonal changes in behavior.

The most common approach to defining the population of interest relies on political boundaries. For example, Bastos et al. (2016) modeled human impacts to the population of Eurasian skylark (*Alauda arvensis*) in a 21,515-km^2 area of northern Portugal that was delineated by the country's boundaries. Likewise, political boundaries have been used to define the population of interest in studies of the impacts of wind energy facilities on wildlife. In a few of these cases, the population of interest has been defined to include all Egyptian vultures (*Neophron percnopterus*) in peninsular Spain (Carrete et al. 2009), all red kites (*Milvus milvus*) in a single German state (Bellebaum et al. 2013), or all red kites in Switzerland (Schaub 2012). In these cases, numerical estimates of population size are often based on survey data collected exclusively within those regions. Defining biological populations based on political boundaries often addresses goals of funding agencies, but this approach is only useful in some specific cases (i.e., Arrondo et al. 2018) and can introduce bias because it often ignores movements across those boundaries.

Other ways to define the population of interest are more biologically based. The simplest approach assumes that the model applies to the entire population of a given species or subspecies. Some of the earliest applied population models for structured populations used such a framework (e.g., Crouse et al. [1987] never really defined the population of interest, Doak [1995] considered an entire disjunct population). More recently, models of the effects of bat fatalities from wind turbines also have considered continent- or country-wide populations (Erickson et al. 2016, Frick et al. 2017). However, it is not always appropriate to define the population of interest as all individuals of a population or species because most stressors only threaten a subset of the population (Diffendorfer et al. 2017). When that subpopulation is small or easily censused, such an approach is straightforward (Freeman et al. 2014). In other situations, defining the appropriate subpopulation creates challenges.

A useful way to refine definitions of the population of interest is by interpreting demographic or ecological data to infer the origins of affected individuals. At the most basic level, this entails using information on the distribution and abundance of species affected by a stressor to inform population estimates. For example, most species of birds shot on islands in the Mediterranean do not breed on those islands (Panuccio 2005). In this situation, range maps and descriptions of migratory flyways can be used to infer information about the origin of these individuals. More detailed site-specific information, such as prevailing directions of migration and observational records, can also be used to infer information about origins of affected individuals (Desholm 2009). Marking, tracking, or modeling tools also have potential to refine definition of the population of interest and its spatial structure. For example, band recovery databases (USGS Bird Banding Laboratory 2019), species distribution models (Santos et al. 2013), active animal tracking (Bridge et al. 2013), and passive genetic (Clegg et al. 2003, Hull et al. 2008, Ruegg et al. 2014) or isotopic (Hobson and Wassenaar 2018) approaches, have been used to derive origins of sampled individuals and to understand migratory connectivity.

Despite the frequent use of this last set of tools in ecological literature, they are infrequently

applied to assess origins of animals affected by anthropogenic stressors. One of the few exceptions is the recent use of stable hydrogen isotope analysis to estimate a catchment area to describe the origin of migratory bats killed at wind turbines in Germany (Voigt et al. 2012). Isotopes have also been used to ascribe a local or non-local catchment area to wildlife killed at renewable energy facilities (Vander Zanden et al. 2018). Similarly, combinations of genetic markers and isotope techniques have been used to identify the catchment area and origin of bats (Pylant et al. 2016) and birds (Katzner et al. 2017) killed at wind energy facilities.

Once a catchment area is defined, then it is possible to generate estimates for the number of individuals within that area. This is more easily done for some species than others. For example, some states, countries, and NGOs publish estimates of sizes of wildlife populations (Clark et al. 2000, Flather et al. 2009, BirdLife International 2016, PIF 2019). The quality of these estimates varies dramatically, with some based on expert opinion and others derived from empirical data. Regardless, the spatial extent of these estimates may closely approximate the distribution of the population of interest. In these cases, those data are directly relevant to population estimation in applied settings. In other cases, including in our examples below, the spatial extent of the population of interest does not match well with the spatial extent of the area for which there is a population estimate. In these situations, population estimates must be modified to create a context-specific and uncertainty-adjusted estimates of the number of individuals within the catchment area that are potentially affected by the stressor. Integrating distributional information derived from demographic or ecological information from the affected individuals, together with estimates of population size, is rarely used to inform estimates of the size of the population of interest. That said, estimates of the number of potentially affected individuals usually are necessary to understand population-level impacts of anthropogenic stressors.

Build rate-based demographic models for the population

Compared to defining the population of interest, it is relatively straightforward to identify demographic parameters and to estimate how

they are affected by anthropogenic stressors. This is because impact assessment is usually achieved through population modeling, and the tools to model biological populations have been applied for nearly a century (Lotka 1920, Volterra 1926, Caswell 2001). Typical modern models require marking animals (mark–recapture models; White and Burnham 1999), or tracking individuals (individual-based models; Shugart et al. 1992, DeAngelis and Mooij 2005), populations (simulation models; Katzner et al. 2006), or vital rates (Leslie matrix models, Caswell 2001; or their Bayesian equivalents, Link and Barker 2010, Kéry and Schaub 2011, Zipkin and Saunders 2018). Any of these monitoring and modeling approaches would be suitable for use in our framework, and the choice of the best approach is likely context-specific (Besbeas et al. 2002, Williams et al. 2002).

The decision regarding which vital rates to assess is important especially because parameter choice can influence conclusions about population dynamics (Cook and Robinson 2017). Anthropogenic effects to populations are most frequently estimated by changes in rates of population growth (lambda or λ; Schaub 2012, Grükorn et al. 2017), adult survival or mortality (Carrete et al. 2009, Bellebaum et al. 2013, Erickson et al. 2015, 2016, Bastos et al. 2016, O'Brien et al. 2017), or probability of extinction (or its derivatives; Frick et al. 2017). Other parameters less often considered include reproductive output (Steenhof et al. 2014) or age ratios (Balbontín et al. 2003). Demographic parameters such as immigration, emigration, and pre-adult reproductive rates are sometimes incorporated into models to refine parameter estimation and predictive accuracy but are rarely used to assess impacts of stressors on populations. However, regardless of the demographic rate under consideration, caution must be used when interpreting model outputs, since rates vary among populations and regions (Rushing et al. 2017, Saunders et al. 2019). It follows that application of rates that are inaccurate or irrelevant for the population of interest can produce model outputs meaningless to that population (White 2000).

Finally, although population size is of key importance to most managers, it is rarely incorporated into rate-based demographic models. However, demographic models can be parameterized

with estimates of vital rates and current population sizes. Projections from these models can then be the basis for estimating changes in population size caused by the stressor. Applying vital rates to numerical estimates is an essential step in the process of upscaling from individually based count data to population-level consequences.

Assess the significance to the population of the rate changes brought on by the stressor

Simulation models, PVAs, and similar tools are established approaches that allow forecasting of population declines. Likewise, there is also a set of metrics that can be applied to demographic rates specifically to define the population-level consequence of a stressor. One such metric is estimated by potential biological removal (PBR; Wade 1998, Runge et al. 2009, Bellebaum et al. 2013, Diffendorfer et al. 2017, Zimmerman et al. 2019). PBR is defined as a fixed harvest rate that may be applied to a population, while allowing that population to reach or maintain some optimum (Runge et al. 2009, Diffendorfer et al. 2017) or without causing extinction (O'Brien et al. 2017). However, PBR has been criticized because of its reliance on weakly founded assumptions, because it considers allowable take from all human-caused fatality sources rather than a single source of interest, and because even PBR-informed take can cause population declines (Green et al. 2016).

Two other approaches to understanding the demographic significance of anthropogenic impacts are acceptable biological change (ABC) and decline probability difference (DPD; Green et al. 2016, Cook and Robinson 2017). ABC estimates the amount of anthropogenic take that results in a 33% probability of a defined population target being achieved (Cook and Robinson 2017). This metric has been criticized because it deals poorly with uncertainty and because the 33% threshold is adapted from another field (from the climate change guidelines detailed in Mastrandrea et al. 2010). As such, it may be arbitrary relative to biologically meaningful thresholds at which anthropogenic take becomes unsustainable (Green et al. 2016, Cook and Robinson 2017). DPD compares the probability that a population would decline in scenarios with and without a single anthropogenic stressor. Like ABC, DPD also is subject to criticism due to its reliance on difficult-to-estimate probabilities and its failure to effectively deal with uncertainty (Green et al. 2016, Cook and Robinson 2017).

A potentially more robust way to identify whether impacts are relevant to conservation of populations is a ratio-based comparison of scenarios derived from population models with and without the anthropogenic stressor (i.e., a counterfactual of impacted and unimpacted populations or CIU, in Cook and Robinson 2017). The ratio-based approach of CIU is an extension of comparisons (not ratios) that have been conducted with parameters such as density of adults (Bastos et al. 2016) or probability of extinction (Carrete et al. 2009), and among different management scenarios (Schaub 2012). Initially proposed exclusively for matrix models and a single parameter, population size (Green et al. 2016), counterfactual ratios may also be implemented for other demographic rate parameters (Cook and Robinson 2017). Furthermore, if paired with a sensitivity analysis, the CIU could provide important insight in situations where field data are limited and effect measurement uncertain, as is often the case when wildlife are affected by anthropogenic stressors. Proponents of CIU argue that it is superior to other approaches because it depends on fewer assumptions, avoids artificial thresholds, and, because it is based on estimation of a ratio of two similar models, it is relatively robust to mis-specification of model input parameters (Green et al. 2016). However, assumptions about the consequences of anthropogenic stressors are only inherent in one of the two models used to generate the ratio, and if those assumptions are violated, then the overall CIU output metric itself may be biased. Furthermore, when evaluating a CIU (or any other ratio), it is important to be clear as to assumptions about the degree to which anthropogenic fatalities are additive or compensatory.

APPLICATION

Application of our proposed framework is context-specific. Thus, to illustrate how context interacts with the framework, we provide examples of its application for two terrestrial species affected by different anthropogenic stressors. We chose these species because they vary in their global population size, in the size of their

geographic distributions, in their ecology, in the anthropogenic stressor that affects them, in the quality of the data available with which to build population models, and in the manner with which we define each species' catchment area. Thus, these two species illustrate some of the flexibility and generality of this framework, as well as some of the data and assumptions it requires. Our first example is for a range- and movement-restricted species for which we use extrinsic information to define the catchment area and a combination of extrinsic and intrinsic information to estimate the number of potentially affected individuals. Our second example is for a species with more complex distribution and movement patterns and for which we use a combination of extrinsic and intrinsic information to define both the catchment area and the size of the potentially affected population.

Greater roadrunners affected by solar energy in the Mojave Desert

Solar energy is rapidly being developed in residential and commercial settings as an alternative to fossil fuels-based energy (O'Shaughnessy et al. 2018). It is also established that its implementation has environmental consequences (Hernandez et al. 2014) for land use, habitat fragmentation (Hernandez et al. 2015), and wildlife (Walston et al. 2016). There are two major types of systems predominantly used in utility-scale solar energy generation (Hernandez et al. 2014). These are photovoltaic (PV), which converts sunlight into electrical current, and concentrating solar (CS), which uses reflective surfaces to focus sunlight and heat a fluid. CS installations sometimes cause wildlife fatalities through collision or burning (Walston et al. 2016). At PV installations in the Mojave Desert, waterbirds and other species are killed when they collide with or land on solar panels (Walston et al. 2016).

The greater roadrunner (*Geococcyx californianus*) is a ground-dwelling, non-migratory, avian predator (Hughes 2011) that sometimes dies at solar facilities in the southwestern United States. Unlike other species, roadrunners are thought not to be killed by the solar facility itself, but instead are found dead along fences and of unknown causes (HT Harvey and Associates 2015). Although the numbers of individuals found are somewhat low (*n* = 14 carcasses in one

year at one facility; HT Harvey and Associates 2015), the unknown cause of their death and their limited dispersal abilities (Unitt 2004) have focused more attention on the species than might be given to a broader ranging species that died of identifiable causes. We applied the five steps of our framework to estimate the population-level consequences of roadrunner fatalities at five solar energy facilities in the Mojave Desert of southern California. Our process is outlined below and detailed in Appendix S1.

Framing the problem.—Although we did not consult with regional wildlife managers, we felt that management would likely be concerned most with the population of birds that are exposed to risk at solar facilities. Therefore, for the purposes of this example, that subset of birds became our population of interest. We focused analysis of impact on adult survival because this parameter should be directly affected by solar facilities and because, with the demographic modeling approach we use (below), survival was more straightforward to model than was the population growth rate (λ). We chose to assess the significance of change to adult survival in the context of the counterfactual (the CIU), and to improve our inference, we performed a sensitivity analysis on the CIU.

Use field-based count data to quantify the effect of the stressor on individuals.—The limited publicly available fatality data from solar energy facilities rarely include estimates adjusted by scavenger removal rates or searcher detection rates (Conkling et al. 2020). Thus, counts of dead roadrunners substantially undercount the actual number of fatalities. However, because these were the only data available, we used those unadjusted field fatality count data in our analysis. These data suggest ~64 roadrunner fatalities per year over the past 8 yr, across the 5 solar facilities we considered (USFWS, *personal communication*).

Characterize the location and size of the population of interest.—We used an odds ratio assignment process with stable hydrogen isotope data (Appendix S3: Table S1) to characterize the likely region of origin of feathers from 24 roadrunner carcasses from 3 solar facilities (Figs. 2, 3). Because the assignment analysis suggested that most birds were from a region approximately defined by the Mojave Desert Bird Conservation

Region (BCR 33), and because of the limited dispersal capacity of these birds, we constrained the averaged catchment area to the boundaries of that BCR and north of the border with Mexico.

We then used the probability surface derived from the isotope data to modify an estimate of size of the roadrunner population in that BCR (PIF 2019). This modified BCR population estimate is the potentially affected population (N_p in Table 1), and it estimates the number of birds potentially at risk from fatality at solar facilities (53,973; see Fig. 2; Appendices S1, S3: Table S2 for details and justification).

Build rate-based demographic models for the population.—We built an age-structured Bayesian integrated population model (IPM) for roadrunners in our catchment area. The model was informed by priors taken from published estimates of roadrunner demography and fit to national-scale bird survey data (Sauer et al. 2017). We used information criteria to determine the best-fit model as our estimate of current conditions (which include fatalities from solar energy). We then multiplied the survival rates from these models by N_p as a means to estimate how many roadrunners survived and died on an annual basis. We repeated this process under current conditions and under conditions without deaths at solar facilities (D_t, D_s, s_a, s_{wos}; Table 1; Appendix S1, Appendix S3: Table S3).

Assess the significance to the population of the rate changes brought on by the stressor.—In this case, with an estimate of 64 annual fatalities, the counterfactual suggests small effects of fatalities at solar facilities on the survival rate of greater roadrunners within BCR 33 (CIU ratio; Table 1). More importantly, our sensitivity analysis suggested that to drop survivorship by 1% requires an additional ~200 fatalities of roadrunners per year, to drop it by 5% would require an additional ~1500 fatalities per year, and to drop it by 10% would require ~3200 fatalities per year (Appendix S3: Table S3). These estimates of effect are conservative, in that they assume that all fatalities are additive.

Although our CIU and sensitivity analysis suggest that the number of fatalities currently is low compared to those required for substantive impacts, they provide a framework to evaluate what level of fatalities may be cause for concern. Because field data were uncorrected for detection and scavenger removal, these fatality counts and the CIU underestimate the actual impact of these fatalities to population-level survival rates. That said, our analysis suggests that even if current estimates are off by an order of magnitude (i.e., if there are actually 640 fatalities/year), this would only cause a ~2% change in survival rates of roadrunners within the BCR. As such, our sensitivity analysis provides a context and potential thresholds for managers to interpret potential increases in numbers of fatalities and to understand the consequences of uncertainty in estimates of mortality rates.

Red-tailed hawks affected by wind turbines in central California

Wind energy development is an anthropogenic stressor that affects many types of terrestrial wildlife (Hutchins and Leopold 2016). Although there are documented indirect effects of wind energy on wildlife, via habitat fragmentation and disturbance, the most obvious and best-studied impact is direct mortality of volant wildlife from striking wind turbine blades (Allison et al. 2019). Among the taxa affected by wind turbines are soaring birds of prey (Watson et al. 2018). The largest and most charismatic of these, such as eagles and griffon vultures, are often of greatest conservation concern, due to their small population sizes and low rates of annual reproduction. As a consequence, these species typically receive the most attention when they are killed at wind energy facilities (de Lucas et al. 2012, Katzner et al. 2017). Nevertheless, large numbers of other species are also affected by wind turbine strikes (ICF International 2016, Thaxter et al. 2017), and the population-level consequences of those fatalities are poorly known.

In California, USA, one of the species most frequently found dead at wind turbines is the red-tailed hawk (*Buteo jamaicensis*; ICF International 2016). Red-tailed hawks have a continent-wide distribution in North America (Preston and Beane 2009), and different subpopulations exhibit a wide variety of migratory behaviors (Bloom et al. 2015). Thus, the birds potentially affected by wind facilities in California likely include in-state, year-round residents, as well as migrant, dispersers, and nomadic individuals from in- or out-of-state. At the same time, it is unlikely that birds from throughout the continental
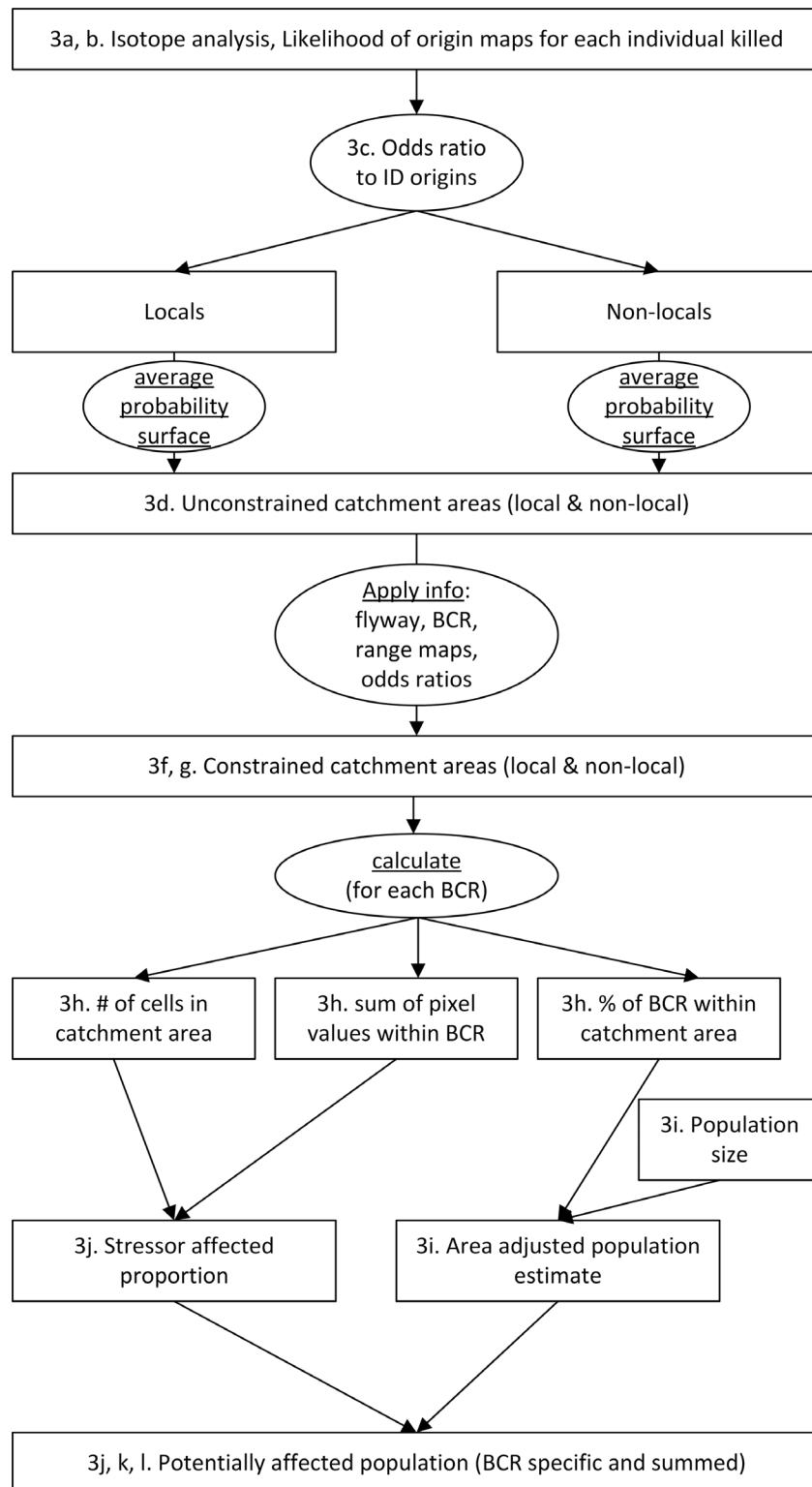
Fig. 2. Flowchart describing the process of characterizing the population of interest in a proposed framework

(Fig. 2. *Continued*)

to assess the consequences of stressors to wildlife. The process starts with likelihood of origin maps for each individual killed and ends with an estimate of the size of the potentially affected population. Numbering and lettering refer to the detailed steps in Appendix S2, step 3 (these are similar but not identical to those in step 3, Appendix S1).

distribution of red-tailed hawks are potentially exposed to wind turbines in California. Therefore, it is important to define a catchment area and identify affected subpopulations, as a precursor to estimating the size of the population of birds potentially affected by fatalities at turbines in the state.

We applied our framework to estimate the population-level consequences of fatalities of red-tailed hawks at a single wind energy complex within California, the Altamont Pass Wind Resource Area (APWRA). Although fatalities at a single facility are unlikely to be as demographically relevant as are cumulative effects across multiple facilities, data from the APWRA are readily available, making this a useful example. Our process is outlined below and detailed in Appendix S2.

Framing the problem.—Once again, our population of interest was that describing the origin of birds killed at turbines at APWRA. We again focused analysis on adult survival and evaluated survival of hawks in the context of the counterfactual.

Use field-based count data to quantify the effect of the stressor on individuals.—Reports of fatalities of red-tailed hawks at APWRA are publicly available for the time period 2005–2013. Unlike in the roadrunner example, studies at APWRA incorporated estimation of detection and scavenging rates. Thus, the data from APWRA have been converted into annual estimates that likely reasonably approximate the number of birds actually killed ($\bar{x}$ = 169/yr; range 133–206; ICF International 2016).

Characterize the location and size of the population of interest.—We evaluated isotope data from 86 red-tailed hawks killed at APWRA (Appendix S3: Table S4), although we used those data differently here than in the prior example. We again used an odds ratio assignment process with stable hydrogen isotope data first to identify 33 birds as being of local origin and 53 as being of non-local origin (Figs. 2, 4). For the non-

local birds, we again used an odds ratio approach to identify their region of greatest likelihood of origin (Fig. 4). We constrained that region by the boundaries of the species' distribution and of the Pacific and Central Flyways. Within that constrained catchment area, we used the probability surface derived from the isotope data from non-local birds to modify BCR-specific estimates of the number of potentially affected non-local birds (Figs. 2, 4; Appendices S2, S3: Table S5). We summed these modified BCR-specific population estimates to generate an estimate of the number of potentially affected birds in the non-local catchment area.

To estimate the size of the potentially affected local population, because the boundaries of BCR #32 aligned closely with the isotope-defined local catchment area, we assumed 100% overlap between the two. We then used the surface derived from the isotope data from the birds characterized as local in origin to modify population estimates for BCR #32 to estimate the size of the potentially affected population within the BCR.

This process resulted in estimates of 605,484 and 98,217 potentially affected red-tailed hawks within the non-local and local catchment areas, respectively (Appendix S3: Table S5). Thus, in total we estimate that there are 703,701 total birds potentially affected by this stressor.

Build rate-based demographic models for the population.—We built separate age-structured Bayesian integrated population models (IPM) for the two potentially affected red-tailed hawk populations (local and non-local). Models were constructed and evaluated as before and we again multiplied modeled rates by population estimates. This allowed us to estimate how many hawks from each catchment area would have died on an annual basis and under scenarios with and without fatalities at APWRA (Table 1; Appendix S3: Table S6).

Assess the significance to the population of the rate changes brought on by the stressor.—Once again, the CIU suggested relatively minor impacts of
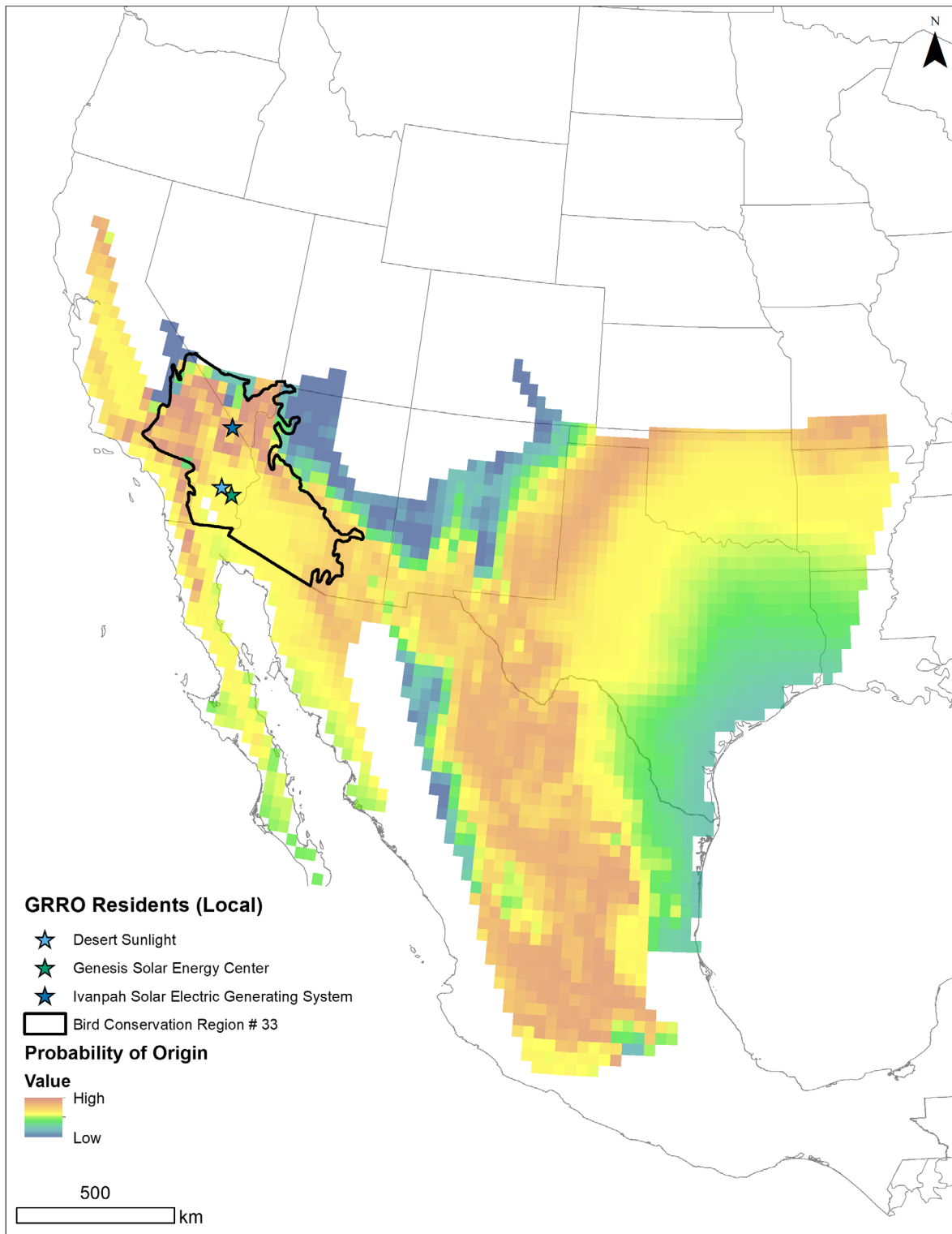
Fig. 3. Map illustrating the process of identifying the catchment area for the population of greater roadrunners

(Fig. 3. *Continued*)

(GRRO) killed at 3 solar facilities in California (Desert Sunlight, Genesis Solar Energy, and Ivanpah Solar Energy Generation System, indicated by blue-green stars on the map). The map illustrates the averaged probability of origin for 26 birds killed at these facilities between 2015 and 2017. The probability surface is restricted to the range of the species in North America (BirdLife International and Handbook of the Birds of the World 2016) and is overlaid by the outline of Bird Conservation Region 33, where all the facilities were located.

Table 1. Input data and modeled evaluation of population-level consequences of anthropogenic stressors on two species of wildlife.

Species	Potentially affected population (N_p)	All deaths/ year in catchment area (D_t)	Deaths from stressor (D_s)	Other deaths (D_o)	Current survival (s_a)	Survival without stressor (s_{wos})	CIU ratio (s_{wos}/s_a)
GRRO, all	53,973	20,996	64†	20,932	0.6110	0.6120	1.002
RTHA, local	98,217	20,134	64	20,070	0.7950	0.7956	1.001
RTHA, non-local	605,484	124,124	105	124,019	0.7950	0.7951	1.000

Notes: Considered here are local populations of greater roadrunners (GRRO) affected by fatalities at solar energy facilities in the Mojave Desert and both local and non-local populations of red-tailed hawks (RTHA) affected by fatalities at the Altamont Pass Wind Resource Area (APWRA). Source information for each column is described in the main text and the Appendices. The CIU ratio is a counterfactual, the ratio of the survival without current mortality from solar to the survival in the current state with mortality from solar.

† Estimates of deaths from solar energy in the Mojave Desert are from count data that do not appear to be based on systematic surveys and include no correction for detection probability or scavenger removal. As a consequence, these estimates likely undercount the actual number of fatalities.

the APWRA on the populations of red-tailed hawks in both the local and the non-local catchment areas (Table 1). Nevertheless, the effect of wind energy was predicted to be slightly stronger on the local population than the non-local populations. The sensitivity analysis (Appendix S3: Table S6) reflected this reality, suggesting that if the true number of fatalities from the non-local population was 5000 individuals, survivorship for that population would be only 1.0% lower than current estimates. In contrast, if all those 5000 fatalities came from the smaller local population, survival would be reduced by 6.4%. We can also use isotope data to inform assignment of fatalities and thus risk assessment for local and non-local populations. For example, in a scenario where 5000 fatalities occurred, the current isotope data suggested that 38% (1900 individuals) would be local birds and 62% (3100 individuals) non-local. In this scenario, the CIU suggests survivorship reductions of 2.4% in the local population and 0.06% in the non-local population. Again, these estimates conservatively assume additive mortality.

Red-tailed hawks are probably the most numerous raptor in California, but also among the species most commonly killed at wind facilities within the state (Watson et al. 2018). Although the true number of fatalities within the state is unknown, the combined effect of many different facilities is likely large. As such, when viewed from the perspective of the combined isotope and demographic analyses, these additional fatalities suggest the potential for demographic consequences for local (California) red-tailed hawk populations.

RELEVANCE, GAPS, AND NEXT STEPS FOR FURTHER FRAMEWORK DEVELOPMENT

Although our framework does not suggest substantial impact from these sources of anthropogenic fatality for either red-tailed hawks or for roadrunners, the potential for effects to the local population of red-tailed hawks suggested by the sensitivity analysis was, perhaps, surprising. This is despite the fact that red-tailed hawks are probably the most abundant and evenly distributed raptor in North America. In contrast, greater roadrunners are a range-restricted species with very specific habitat requirements and a substantially smaller overall population size. As such, our examples illustrate the utility of assessing population consequences
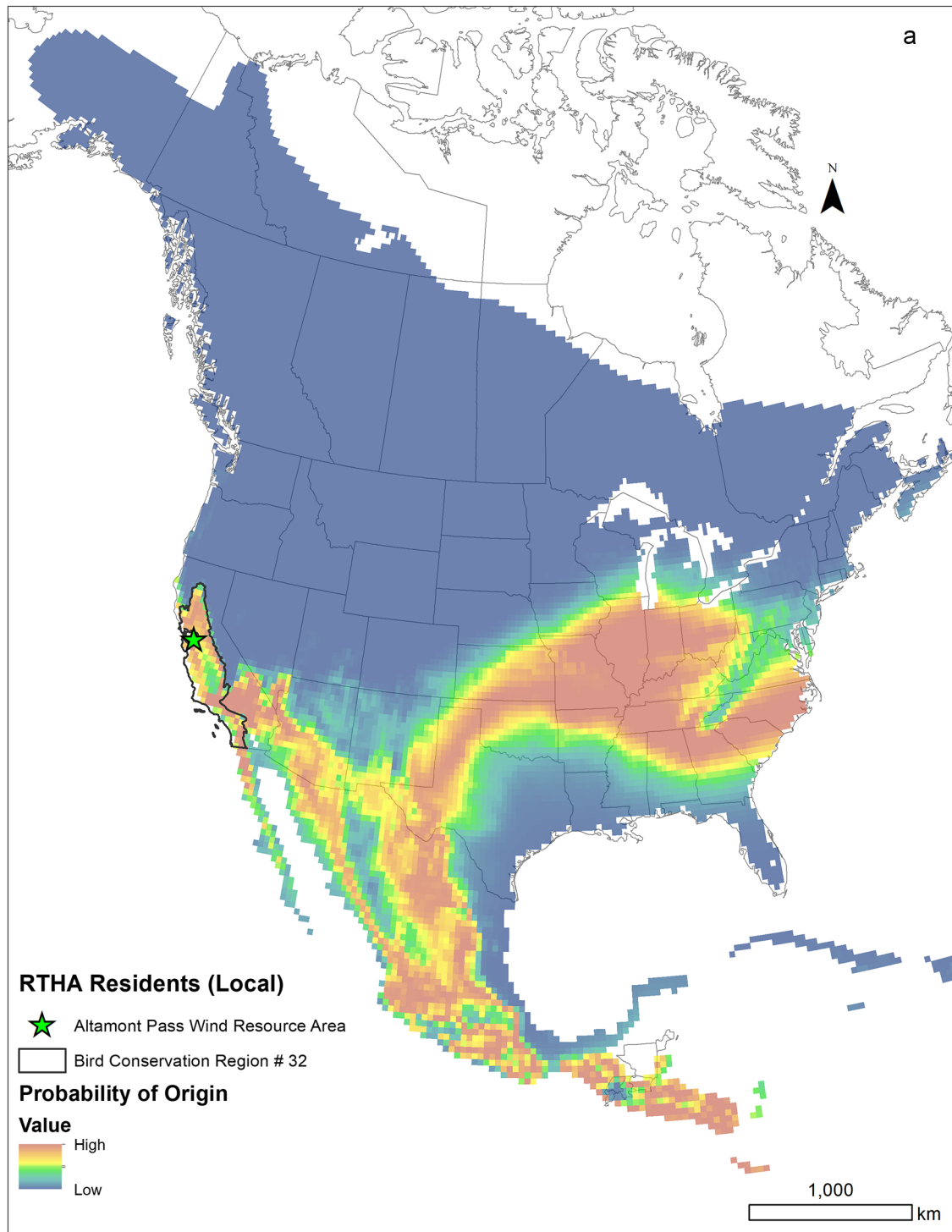
Fig. 4. Maps illustrating the process of identifying the catchment area for the population of red-tailed hawks (RTHA) killed at Altamont Pass Wind Resource Area (APWRA; location indicated by the green star) in California. The maps illustrate the averaged probability of origin for (a) 33 local and (b) 53 non-local birds killed at APWRA between 2005 and 2017. The probability surfaces are restricted to the range of the species in North

(Fig. 4. *Continued*)

America (BirdLife International and Handbook of the Birds of the World 2016) and are overlaid on numbered Bird Conservation Regions. The solid black line in panel (a) is the boundary of BCR 32; in panel (b), it demarcates the boundaries of the odds ratio-defined "constrained catchment area" for (a) local and (b) non-local hawks killed at APWRA. The catchment area for local birds is restricted to the BCR in which APWRA is located (BCR 32). The catchment area for non-local birds covers several BCRs; the dotted line running north–south in (b) is the boundary between the Central Flyway (to the west) and the Mississippi Flyway (to the east).

of anthropogenic stressors in a framework that incorporates (1) information about the location of, and population density within, a catchment area; (2) local vs. non-local origin assignment; and (3) sensitivity analysis of an impact metric (here the CIU). These first two especially were critical to upscaling from count-based data on individuals to rate-based population-level inference and the third for exploring consequences of fatalities across multiple facilities. That said, despite its usefulness, there is room for improvement of the framework, in terms of both the implementation process and the technical tools it uses.

Strengths, challenges, and process-based areas for improvement

A strength of this framework is its broad applicability. In particular, it accommodates most terrestrial wildlife species, movement strategies, or geographic distributions, most anthropogenic stressors or combinations of stressors, most mechanisms to define a catchment area, and most consequences to species, whether direct or indirect. As an example, the framework was informative for the two species of birds we considered, even though they have dramatically different life histories, ecological relationships, and behaviors, and they were affected by different stressors at different spatial scales. Furthermore, although there is reasonably good demographic and fatality data for red-tailed hawks, both the demographic data and the fatality data are poor for roadrunners. In spite of these differences, the framework allowed us to draw some level of inference about effects of stressors on both species and, probably more importantly, provided insight into conservation outcomes in potential future scenarios.

Perhaps the greatest challenges to implementing this framework are in the areas where it is most novel—in using information about the catchment area to upscale from individually based count data to rate-based population-level estimates. In our example, where we paired isotope- or BCR-defined catchment areas with BCR-derived and isotope-modified estimates of population size, these challenges manifested themselves in the mismatch between the boundaries of the catchment area and boundaries of the BCRs. Furthermore, these challenges were different for the highly mobile red-tailed hawk than for the largely local greater roadrunner. These inter-species differences are likely not unique and will likely occur regardless of the species considered and regardless of the probabilistic method used to define the catchment area. As such, there is an important need to develop conceptual and methodological tools to pair probabilistically defined catchment areas with population estimates defined at different spatial scales. Especially for highly mobile species, accurate identification of a catchment area likely requires (1) adaptation of probabilistic statistical approaches to interpret the data produced by genetic, isotope, or other approaches that generate probability surfaces and (2) incorporation of external information on flyways, distribution, habitat specialization, migration behavior, and management.

The transition from count-based to rate-based estimates was also influenced by a number of simplifying assumptions we made. For example, we assumed that red-tailed hawks from BCRs in the eastern part of the non-local catchment area (e.g., Montana) were equally likely to be exposed to risk in California as were individuals in BCRs in the western part of that same catchment area (e.g., Nevada). That is unlikely to be the case, and it would make sense to use a distance-weighted metric to further adjust our BCR-specific population estimates prior to making management decisions.
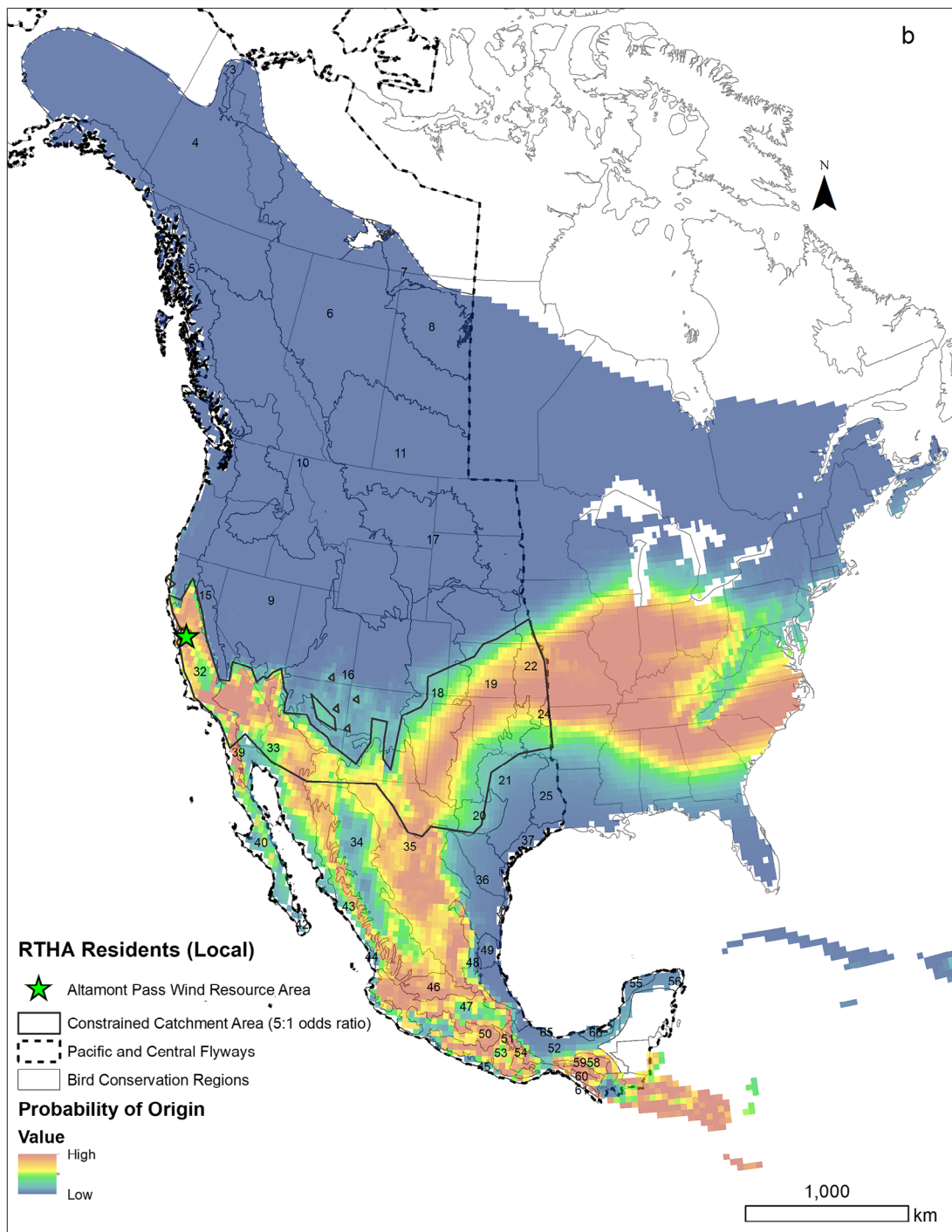
(Fig. 4. *Continued*)

Similarly, assumptions we made to estimate the extent of catchment area for the hawks influenced the outcome of that analysis. First, we used an odds ratio assignment process with stable hydrogen isotope data to define the boundaries of catchment area. Such a technique

is conservative in that it ensures that the majority of birds potentially at risk are included in our population estimate. However, being conservative in this way is risky with regard to conservation outcomes because, if the actual size of the affected population is smaller than that identified (i.e., the animals come from a smaller area than estimated by the odds ratio), then the demographic effect of fatalities may be larger than estimated. Thus, in many settings, being more cautious in estimating population size may be appropriate. Second, we assumed that all non-local birds could be described by a single probability-of-origin map. In fact, the stable isotope data suggest that some of the red-tailed hawk fatalities we considered likely came from areas south of APWRA and others from areas to the north (see Katzner et al. 2017 for an example of how such geographic assignments can be approximated). Future work could incorporate multiple probability-of-origin maps for non-local birds, each clustered by area of origin. This would then allow development of separate population models that would allow assessment of the effects of spatial structure and demographic differences among the populations of origin (e.g., how do the population-level consequences of fatalities differ if they are composed of 25% vs. 75% northern red tails).

A second challenge to implementation of this framework is in data availability. This plays out in at least three ways. First, although range maps and population estimates are available for many of the world's bird species (BirdLife International and Handbook of the Birds of the World 2016), the accuracy and precision of those maps and estimates vary by region and species. Likewise, similar data often are not available for other wildlife species, and there are very limited data for some taxa such as invertebrates (Dopheide et al. 2019). Furthermore, in cases where those data are available, they may not be estimated in a way that allows them to be effectively matched to a probabilistically defined catchment area. Second, data are often lacking to describe the consequence of a stressor on wildlife. In the case of fatalities and other direct effects, these gaps can also be addressed through increased monitoring or, in a few cases, through increased availability of existing data. However, in the case of indirect effects,

addressing these gaps may require substantial research effort and scientific advances. Third, our population modeling used the best available demographic information as Bayesian priors. However, for wide-ranging species, demographic rates often vary across their range, and we could not match demographic rates to the regions we modeled. Thus, a demographic rate reported from a study in Texas may not be appropriate for a population model for animals in California. That being the case, this framework could be improved by development of spatially explicit demographic models that reflect ecological variation across the catchment area.

A third challenge to implementing this framework lies in constraints in our data collection. For example, the tools used to establish migratory connectivity or to link affected individuals to catchment areas (isotopes, genetics, telemetry, dataloggers) often are imprecise or difficult to apply after an individual is affected or killed. These tools all provide more information than historically was available for managers to make decisions. That said, imprecision in the estimate of catchment area size may have a dramatic influence on population estimates and thus on estimates of the consequence of a particular stressor to a species. This observation highlights the importance of developing tools that more precisely identify origins of migratory individuals, especially those that are sampled after being affected or killed by anthropogenic stressors. Likewise, all these techniques require substantial initial investment, either to build reference datasets or to trap and track animals, before assessments are made. Integration of multiple types of data is one way to increase the precision of these tools (Clegg et al. 2003, Kelly et al. 2005, Paxton et al. 2013, Rundel et al. 2013, Nelson et al. 2015). However, work in this area is still in the early stages and it requires further development.

Technical areas for improvement

There also are several technical areas in which we think the framework can be improved. In particular, improvements could be made in handling process uncertainty, sublethal effects, and non-point sources of stress. Although uncertainty is addressed via the Bayesian population models and the sensitivity analysis for the CIU, there is

ample room to address uncertainty in other steps in our framework. Likewise, although we only focused on lethal effects to wildlife, sublethal effects often are demographically relevant and the framework could be improved by incorporating those impacts. Finally, our work evaluated consequences of two point sources of mortality. There may be additional challenges to using this framework to understand the effects of non-point, broadly distributed, threats such as those from environmental toxins or window strike, both of which can influence large numbers of wildlife across a very large landscape.

Finally, our Bayesian modeling framework has a number of constraints. Although effective at dealing with uncertainty, these models can be difficult to implement simultaneously for multiple species. Because our modeling approach focused exclusively on survival, we may have missed demographic effects related to other processes. Building models that incorporate effects on other parameters, especially population growth rate or population size, is therefore an important research need. Furthermore, the models we implemented ignored immigration, emigration, density dependence, and Allee effects. Likewise, they make at least two simplifying assumptions—that fatalities caused by an anthropogenic stressor were additive and that there were no temporal patterns or age structure within the fatalities. Addressing these types of issues is of high priority in the field of population ecology (Caswell 2001), and integrating improvements in these areas would improve this framework.

Real-world implementation

Although the two examples we provide are focused on renewable energy, the framework we develop here should be broadly applicable in a wide range of circumstances. For example, roadway mortality is an important source of fatalities of birds (Loss et al. 2014*b*), insects (Baxter-Gilbert et al. 2015), terrestrial (Visintin et al. 2017) and volant mammals (Fensome and Mathews 2016), and amphibians (Hamer et al. 2015). In each of these situations, our framework could be applied to understand population-level consequences of these fatalities. As an example, stable isotope tools similar to those we describe here were used, albeit without the demographic context we

apply, to show that the 2009 crash of US Airways Flight 1549 in New York, USA, was caused by geese that were migratory, not local, in origin (Marra et al. 2009).

Implementation of this framework is dependent, in at least two stages, on information from conservation practitioners and other stakeholders (Fig. 1). In particular, stakeholders have an important role in deciding how to define focal species and the population of interest. As such, those decisions and the goals of the end user can dramatically influence the outcomes of this process. For example, when defining a potentially affected population, an end user who is an ecologist may focus on groups of animals defined as evolutionary or ecologically significant units. In contrast, an end user who is a wildlife or land manager may instead focus on animals within a biologically arbitrary but management-relevant political boundary. Depending on the questions being asked, either may be an appropriate definition of the populations of interest. Furthermore, although the BCR and stable isotope approaches we used to define a catchment area were biologically meaningful, this approach may not always align with management goals. As such, in other situations, the catchment area could be defined with other probabilistic or non-probabilistic tools. Thus, defining the population of interest so that it is relevant to management decisions is of primary importance to bridging the research-implementation gap that can bedevil translation of research information into conservation action.

Conclusions

The framework outlined here has potentially broad applicability for addressing the population-level effects of anthropogenic stressors on terrestrial wildlife. The types of approaches we suggest using are well established, but our framework provides a novel, management-relevant unification of these separate tools. This framework is also largely platform independent—it can accommodate different definitions of populations of interest, different tools to estimate catchment areas, different types of population models, and even different evaluations of its effectiveness. Perhaps its greatest limitation though is in the availability of suitable field data

that estimate numbers of individuals affected, population sizes, and demographic parameters. Thus, as data quality improves, we anticipate this framework will become more generally useful and its predictions more accurate.

LITERATURE CITED

Adams, V. M., M. Mills, R. Weeks, D. B. Segan, R. L. Pressey, G. G. Gurney, C. Groves, F. W. Davis, and J. G. Álvarez-Romero. 2019. Implementation strategies for systematic conservation planning. Ambio 48:139–152.

Allison, T. D., et al. 2019. Impacts to wildlife of wind energy siting and operation in the United States. Issues in Ecology 21:1–24.

Arnett, E. B., and E. F. Baerwald. 2013. Impacts of wind energy development on bats: implications for conservation. Pages 435–456 in R. A. Adams and S. C. Pedersen, editors. Bat evolution, ecology, and conservation. Springer Science + Business Media, New York, New York, USA.

Arrondo, E., M. Moleón, A. Cortés-Avizanda, J. Jiménez, P. Beja, J. A. Sánchez-Zapata, and J. A. Donázar. 2018. Invisible barriers: Differential sanitary regulations constrain vulture movements across country borders. Biological Conservation 219:46–52.

Balbontín, J., V. Penteriani, and M. Ferrer. 2003. Variations in the age of mates as an early warning signal of changes in population trends? The case of Bonelli's eagle in Andalusia. Biological Conservation 109:417–423.

Bastos, R., A. Pinhanços, M. Santos, R. F. Fernandes, J. R. Vicente, F. Morinha, J. P. Honrado, P. Travassos, P. Barros, and J. A. Cabral. 2016. Evaluating the regional cumulative impact of wind farms on birds: How can spatially explicit dynamic modelling improve impact assessments and monitoring? Journal of Applied Ecology 53:1330–1340.

Baxter-Gilbert, J. H., J. L. Riley, C. J. Neufeld, J. D. Litzgus, and D. Lesbarrères. 2015. Road mortality potentially responsible for billions of pollinating insect deaths annually. Journal of Insect Conservation 19:1029–1035.

Bellebaum, J., F. Korner-Nievergelt, T. Durr, and U. Mammen. 2013. Wind turbine fatalities approach a level of concern in a raptor population. Journal for Nature Conservation 21:394–400.

Besbeas, P., S. N. Freeman, B. J. T. Morgan, and E. A. Catchpole. 2002. Integrating mark-recapture-recovery and census data to estimate animal abundance and demographic parameters. Biometrics 58:540–547.

Bibby, C., N. Burgess, D. Hill, and S. Mustoe. 2000. Bird census techniques. Second edition. Academic Press, London, UK.

BirdLife International and Handbook of the Birds of the World. 2016. Bird species distribution maps of the world. Version 6.0. Available at http://datazone.birdlife.org/species/requestdis

Bloom, P. H., M. D. McCreary, J. M. Scott, J. M. Papp, K. J. Sernka, S. E. Thomas, J. W. Kidd, E. H. Henkel, J. L. Henkel, and M. J. Gibson. 2015. Northward summer migration of red-tailed hawks fledged from southern latitudes. Journal of Raptor Research 49:1–17.

Bonnington, C., K. J. Gaston, and K. L. Evans. 2013. Fearing the feline: Domestic cats reduce avian fecundity through trait-mediated indirect effects that increase nest predation by other species. Journal of Applied Ecology 50:15–24.

Bridge, E. S., J. F. Kelly, A. Contina, R. M. Gabrielson, R. B. MacCurdy, and D. W. Winkler. 2013. Advances in tracking small migratory birds: a technical review of light-level geolocation. Journal of Field Ornithology 84:121–137.

Carrete, M., J. A. Sánchez-Zapata, J. R. Benítez, M. Lobón, and J. A. Donázar. 2009. Large scale risk-assessment of wind-farms on population viability

of a globally endangered long-lived raptor. Biological Conservation 142:2954–2961.

Caswell, H. 2001. Matrix population models. Sinauer Associates, Sunderland, Massachusetts, USA.

Clark, J. R., et al. 2000. North American Bird Conservation Initiative: bird conservation region descriptions, a supplement to the North American Bird Conservation Initiative Bird Conservation Regions Map. US NABCI committee.

Clegg, S. M., J. F. Kelly, M. Kimura, and T. B. Smith. 2003. Combining genetic markers and stable isotopes to reveal population connectivity and migration patterns in a Neotropical migrant, Wilson's warbler (*Wilsonia pusilla*). Molecular Ecology 12:819–830.

Cohen, E. B., J. A. Hostetler, M. T. Hallworth, C. S. Rushing, T. S. Sillett, and P. P. Marra. 2018. Quantifying the strength of migratory connectivity. Methods in Ecology and Evolution 9:513–524.

Conkling, T. J., S. R. Loss, J. E. Diffendorfer, A. Duerr, and T. E. Katzner 2020. Limitations, lack of standardization, and recommended best practices in studies of renewable energy effects on birds and bats. Conservation Biology. https://doi.org/10.1111/cobi.13457.

Cook, A. S., M. Parsons, I. Mitchell, and R. A. Robinson. 2011. Reconciling policy with ecological requirements in biodiversity monitoring. Marine Ecology Progress Series 434:267–277.

Cook, A. S. C. P., and R. A. Robinson. 2017. Towards a framework for quantifying the population-level consequences of anthropogenic pressures on the environment: the case of seabirds and windfarms. Journal of Environmental Management 190:113–121.

Crouse, D. T., L. B. Crowder, and H. Caswell. 1987. A stage-based population model for loggerhead sea turtles and implications for conservation. Ecology 68:1412–1423.

Dalthorp, D., L. Madsen, M. Huso, P. Rabie, R. Wolpert, J. Studyvin, J. Simonis, and J. Mintz. 2018. GenEst statistical models—A generalized estimator of mortality. Chapter 2 Section A *in* U.S. Geological Survey Techniques and Methods. Book 7. US Geological Survey, Corvallis, Oregon, USA.

DeAngelis, D. L., and W. M. Mooij. 2005. Individual-based modeling of ecological and evolutionary processes. Annual Review of Ecology, Evolution, and Systematics 36:147–168.

de Lucas, M., M. Ferrer, M. J. Bechard, and A. R. Muñoz. 2012. Griffon vulture mortality at wind farms in southern Spain: distribution of fatalities and active mitigation measures. Biological Conservation 147:184–189.

Desholm, M. 2009. Avian sensitivity to mortality: prioritising migratory bird species for assessment at proposed wind farms. Journal of Environmental Management 90:2672–2679.

Diffendorfer, J. E., J. A. Beston, M. D. Merrill, J. C. Stanon, M. D. Corum, S. R. Loss, W. E. Thogmartin, D. H. Johnson, R. A. Erickson, and K. W. Heist. 2017. A method to assess the population-level consequences of wind energy facilities on bird and bat species. Ch. 4. *In* J. Köppel, editor. Wind energy and wildlife interactions. Springer, Berlin, Germany.

Doak, D. F. 1995. Source-sink models and the problem of habitat degradation: general models and applications to the Yellowstone grizzly. Conservation Biology 9:1370–1379.

Dopheide, A., et al. 2019. Estimating the biodiversity of terrestrial invertebrates on a forested island using DNA barcodes and metabarcoding data. Ecological Applications 29:e01877.

Erickson, R. A., E. A. Eager, J. C. Stanton, J. A. Beston, J. E. Diffendorfer, and W. E. Thogmartin. 2015. Assessing local population vulnerability with branching process models: an application to wind energy development. Ecosphere 6:254.

Erickson, R. A., W. E. Thogmartin, J. E. Diffendorfer, R. E. Russell, and J. A. Szymanski. 2016. Effects of wind energy generation and white-nose syndrome on the viability of the Indiana bat. PeerJ 4:e2830.

Fensome, A. G., and F. Mathews. 2016. Roads and bats: a meta-analysis and review of the evidence on vehicle collisions and barrier effects. Mammal Review 46:311–323.

Flather, C. H., M. S. Knowles, and S. J. Brady. 2009. Population and harvest trends of big game and small game species: a technical document supporting the USDA Forest Service Interim Update of the 2000 RPA Assessment. Gen. Tech. Rep. RMRS-GTR-219. U.S. Department of Agriculture, Forest Service, Rocky Mountain Research Station, Fort Collins, Colorado, USA.

Freeman, S., K. Searle, M. Bogdanova, S. Wanless, and F. Daunt. 2014. Population dynamics of Forth & Tay breeding seabirds: review of available models and modelling of key breeding populations. Final report to Marine Scotland Science. CEH, UK.

Frick, W. F., E. F. Baerwald, J. F. Pollock, R. M. R. Barclay, J. A. Szymanski, T. J. Weller, A. L. Russell, S. C. Loeb, R. A. Medellin, and L. P. McGuire. 2017. Fatalities at wind turbines may threaten population viability of a migratory bat. Biological Conservation 209:172–177.

Green, R. E., R. H. W. Langston, A. McCluskie, R. Sutherland, and J. D. Wilson. 2016. Lack of sound science in assessing wind farm impacts on seabirds. Journal of Applied Ecology 53:1635–1641.

Greenberg, R., and P. P. Marra, editors. 2005. Birds of two worlds: the ecology and evolution of migration. Johns Hopkins University Press, Baltimore, Maryland, USA.

Griesser, M., et al. 2017. Experience buffers extrinsic mortality in a group-living bird species. Oikos 126:1258–1268.

Grükorn, T., J. Blew, O. Krüger, A. Potiek, M. Reichenbach, von Rönn J., H. Timmermann, S. Weitekamp, and G. Nehls. 2017. A large-scale, multispecies assessment of avian mortality rates at land-based wind turbines in Northern Germany. Ch. 3. *In* J. Köppel, editor. Wind Energy and Wildlife Interactions. Springer, Berlin, Germany.

Hamer, A. J., T. E. Langton, and D. Lesbarrères. 2015. Making a safe leap forward: mitigating road impacts on amphibians. Handbook of Road Ecology. Wiley, Chichester, UK.

Hayes, M. A. 2013. Bats killed in large numbers at United States wind energy facilities. BioScience 63:975–979.

Hernandez, R. R., M. K. Hoffacker, M. L. Murphy-Mariscal, G. C. Wu, and M. F. Allen. 2015. Solar energy development impacts on land cover change and protected areas. Proceedings of the National Academy of Sciences of USA 112:13579–13584.

Hernandez, R. R., et al. 2014. Environmental impacts of utility-scale solar energy. Renewable and Sustainable Energy Reviews 29:766–779.

Hobson, K. A., and L. I. Wassenaar. 2018. Tracking animal migration with stable isotopes. Second edition. Academic Press, London, UK.

Hostetler, J. A., T. S. Sillett, and P. P. Marra. 2015. Full-annual-cycle population models for migratory birds. Auk 132:433–449.

HT Harvey and Associates. 2015. Ivanpah Solar Electric Generating System. Avian & Bat Monitoring Plan. 2013-2014 Annual Report (revised). Report to the California Energy Commission for Project # 2802-07.

Hughes, J. M. 2011. Greater Roadrunner (*Geococcyx californianus*), version 2.0. *In* A. F. Poole, editor. The birds of North America. Cornell Lab of Ornithology, Ithaca, New York, USA.

Hull, J. M., A. C. Hull, B. N. Sacks, J. P. Smith, and H. B. Ernest. 2008. Landscape characteristics influence morphological and genetic differentiation in a widespread raptor (Buteo jamaicensis). Molecular Ecology 17:810–824.

Hunt, G. W., J. D. Wiens, P. R. Law, M. R. Fuller, T. L. Hunt, D. E. Driscoll, and R. E. Jackman. 2017. Quantifying the demographic cost of human-related mortality to a raptor population. PLOS ONE 12:e0172232.

Huso, M. M. 2011. An estimator of wildlife fatality from observed carcasses. Environmetrics 22:318–329.

Huso, M. M., and D. Dalthorp. 2014. Accounting for unsearched areas in estimating wind turbine-caused fatality. Journal of Wildlife Management 78:347–358.

Huso, M. M., D. Dalthorp, T. J. Miller, and D. Bruns. 2016. Wind energy development: methods to assess bird and bat fatality rates post-construction. Human-Wildlife Interactions 10:62–70.

Hutchins, M., and B. D. Leopold. 2016. Wildlife and wind energy: Are they compatible? Human-Wildlife Interactions 10:4–6.

ICF International. 2016. Final Report Altamont Pass Wind Resource Area Bird Fatality Study, Monitoring Years 2005–2013. April. M107. (ICF 00904.08.) Sacramento, CA. Prepared for Alameda County Community Development Agency, Hayward, California, USA.

Katzner, T. E., E. A. Bragin, and E. J. Milner-Gulland. 2006. Modelling populations of long-lived birds of prey for conservation: a study of imperial eagles (*Aquila heliaca*) in Kazakhstan. Biological Conservation 132:322–335.

Katzner, T. E., et al. 2017. Golden Eagle fatalities and the continental-scale consequences of local wind-energy generation. Conservation Biology 31:406–415.

Kelly, J. F., K. C. Ruegg, and T. B. Smith. 2005. Combining isotopic and genetic markers to identify breeding origins of migrant birds. Ecological Applications 15:1487–1497.

Kéry, M., and M. Schaub. 2011. Bayesian population analysis using WinBUGS. Academic Press, London, UK.

Link, W. A., and R. J. Barker. 2010. Bayesian inference with ecological applications. Academic Press, London, UK.

Loss, S. R., T. Will, and P. P. Marra. 2012. Direct human-caused mortality of birds: improving quantification of magnitude and assessment of population impact. Frontiers in Ecology and Environment 10:357–364.

Loss, S. R., T. Will, and P. P. Marra. 2014*a*. Refining estimates of bird collision and electrocution mortality at power lines in the United States. PLOS ONE 9: e101565.

Loss, S. R., T. Will, and P. P. Marra. 2014*b*. Estimation of bird-vehicle collision mortality on U.S. Roads. Journal of Wildlife Management 78:763–771.

Loss, S. R., T. Will, and P. P. Marra. 2015. Direct mortality of birds from anthropogenic causes. Annual Review of Ecology, Evolution, and Systematics 46:99–120.

Lotka, A. J. 1920. Analytical note on certain rhythmic relations in organic systems. Proceedings of the National Academy of Sciences of USA 6:410–415.

Maclean, I. M., M. M. Rehfisch, H. Skov, and C. B. Thaxter. 2013. Evaluating the statistical power of detecting changes in the abundance of seabirds at sea. Ibis 155:113–126.

Marra, P. P., C. J. Dove, R. Dolbeer, N. F. Dahlan, M. Heacker, J. F. Whatton, N. E. Diggs, C. France, and G. A. Henkes. 2009. Migratory Canada geese cause crash of US Airways Flight 1549. Frontiers in Ecology and the Environment 7:297–301.

Martin, T. E. 2015. Age-related mortality explains life history strategies of tropical and temperate songbirds. Science 349:966–970.

Mastrandrea, M. D., et al. 2010. Guidance Note for Lead Authors of the IPCC Fifth Assessment Report on Consistent Treatment of Uncertainties. Intergovernmental Panel on Climate Change.

May, R., E. A. Masden, F. Bennet, and M. Perron. 2019. Considerations for upscaling individual effects of wind energy development towards population-level impacts on wildlife. Journal of Environmental Management 230:84–93.

Morris, W., D. Doak, M. Groom, P. Kareiva, J. Fieberg, L. Gerber, P. Murphy, and D. Thomson. 1999. A practical handbook for population viability analysis. The Nature Conservancy, Arlington, Virginia, USA.

Morrison, M. L., and K. H. Pollock. 1997. Development of a practical modeling framework for estimating the impact of wind technology on bird populations. NREL/SR-440-23088. UC Category: 1210. NREL, Golden, Colorado, USA.

Nelson, D. M., M. Braham, T. A. Miller, A. E. Duerr, J. Cooper, M. Lanzone, J. Lemaître, and T. E. Katzner. 2015. Stable hydrogen isotopes identify leapfrog migration, degree of connectivity and summer distribution of Golden Eagles in eastern North America. Condor 117:414–429.

Oberhauser, K., R. Wiederholt, J. E. Diffendorfer, D. Semmens, L. Ries, W. E. Thogmartin, L. Lopez-Hoffman, and B. Semmens. 2017. A trans-national monarch butterfly population model and implications for regional conservation priorities. Ecological Entomology 42:51–60.

O'Brien, S. H., A. S. C. P. Cook, and R. A. Robinson. 2017. Implicit assumptions underlying simple harvest models of marine bird populations can mislead environmental management decisions. Journal of Environmental Management 201:163–171.

O'Shaughnessy, E., J. Heeter, and J. Sauer. 2018. Status and trends in the U.S. Voluntary Green Power Market: 2017 Data. National Renewable Energy Laboratory. NREL/TP-6A20-72204, Golden, Colorado, USA. https://www.nrel.gov/docs/fy19osti/72204.pdf

Panuccio, M. 2005. Protection of migratory raptors in the Mediterranean. Sustainable Mediterranean 35:13–14.

Partners in Flight (PIF). 2019. Population estimates database, Version 3.0. Available at http://pif.birdconservancy.org/PopEstimates

Paxton, K. L., M. Yau, F. R. Moore, and D. Irwin. 2013. Differential migratory timing of western populations of Wilson's Warblers (Cardellina pusilla) revealed by mitochondrial DNA and stable isotopes. Auk 130:689–698.

Preston, C. R., and R. D. Beane. 2009. Red-tailed Hawk (Buteo jamaicensis), version 2.0. In A. F. Poole, editor. The birds of North America. Cornell Lab of Ornithology, Ithaca, New York, USA.

Pylant, C. L., D. M. Nelson, M. C. Fitzpatrick, J. E. Gates, and S. R. Keller. 2016. Geographic origins and population genetics of bats killed at wind-energy facilities. Ecological Applications 26:1381–1395.

Ruegg, K. C., E. C. Anderson, K. L. Paxton, V. Apkenas, S. Lao, R. B. Siegel, D. F. Desante, F. Moore, and T. B. Smith. 2014. Mapping migration in a songbird using high-resolution genetic markers. Molecular Ecology 23:5726–5739.

Rundel, C. W., et al. 2013. Novel statistical methods for integrating genetic and stable isotope data to infer individual-level migratory connectivity. Molecular Ecology 22:4163–4176.

Runge, M. C., J. R. Sauer, M. L. Avery, B. F. Blackwell, and M. D. Koneff. 2009. Assessing allowable take of migratory birds. Journal of Wildlife Management 73:556–565.

Rushing, C. S., J. A. Hostetler, T. S. Sillett, P. P. Marra, J. A. Rotenberg, and T. B. Ryder. 2017. Spatial and temporal drivers of avian population dynamics across the annual cycle. Ecology 98:2837–2850.

Santos, H., L. Rodrigues, G. Jones, and H. Rebelo. 2013. Using species distribution modelling to predict bat fatality risk at wind farms. Biological Conservation 157:178–186.

Sauer, J., D. K. Niven, J. E. Hines, D. J. Ziolowski Jr, K. L. Pardieck, J. E. Fallon, and W. L. Link. 2017. The North American Breeding Bird Survey, Results and Analysis 1966–2015, Version 2.07.2017. USGS Patuxent Wildlife Research Center, Laurel, Maryland, USA.

Saunders, S. P., M. T. Farr, A. D. Wright, C. A. Bahlai, J. W. Ribeiro Jr, S. Rossman, A. L. Sussman, T. W. Arnold, and E. F. Zipkin. 2019. Disentangling data discrepancies with integrated population models. Ecology 100:e02714.

Schaub, M. 2012. Spatial distribution of wind turbines is crucial for the survival of red kite populations. Biological Conservation 155:111–118.

Shugart, H., T. Smith, and W. Post. 1992. The potential for application of individual-based simulation models for assessing the effects of global change. Annual Review of Ecology and Systematics 23:15–38.

Smallwood, K. S., and C. Thelander. 2008. Bird mortality at the Altamont Pass Wind Resource Area, California. Journal of Wildlife Management 72:215–223.

Steenhof, K., J. L. Brown, and M. N. Kochert. 2014. Temporal and spatial changes in golden eagle reproduction in relation to increased off highway vehicle activity. Wildlife Society Bulletin 38:682–688.

Sur, M., J. R. Belthoff, E. J. Bjerre, B. A. Millsap, and T. E. Katzner. 2018. The utility of point count surveys to predict wildlife interactions with wind energy facilities: an example focused on golden eagles. Ecological Indicators 88:126–133.

Thaxter, C. B., G. M. Buchanan, J. Carr, S. H. Butchart, T. Newbold, R. E. Green, J. A. Tobias, W. B. Foden, S. O'Brien, and J. W. Pearce-Higgins. 2017. Bird and bat species' global vulnerability to collision mortality at wind farms revealed through a trait-based assessment. Proceedings of the Royal Society B: Biological Sciences 284:20170829.

Thompson, S. J., D. H. Johnson, N. D. Neimuth, and C. A. Ribic. 2015. Avoidance of unconventional oil wells and roads exacerbates habitat loss for grassland birds in the North American great plains. Biological Conservation 192:82–90.

Unitt, P. 2004. The San Diego county bird atlas. Sunbelt Publications, El Cajon, California, USA.

USGS Bird Banding Laboratory. 2019. North American bird banding and band encounter data set. Patuxent Wildlife Research Center, Laurel, Maryland, USA.

Vander Zanden, H., D. Nelson, M. Wunder, T. Conkling, and T. Katzner. 2018. Application of isoscapes to determine geographic origin of terrestrial wildlife for conservation and management. Biological Conservation 228:268–280.

Visintin, C., R. Van Der Ree, and M. A. McCarthy. 2017. Consistent patterns of vehicle collision risk for six mammal species. Journal of Environmental Management 201:397–406.

Voigt, C. C., A. G. Popa-Lisseanu, I. Niermann, and S. Kramer-Schadt. 2012. The catchment area of wind farms for European bats: a plea for international regulations. Biological Conservation 153:80–86.

Volterra, V. 1926. Fluctuations in the abundance of a species considered mathematically. Nature 118:558–560.

Wade, P. R. 1998. Calculating limits to the allowable human-caused mortality of cetaceans and pinnipeds. Marine Mammal Science 14:1–37.

Walston, L. J. Jr., K. E. Rollins, K. E. LaGory, K. P. Smith, and S. A. Meyers. 2016. A preliminary assessment of avian mortality at utility-scale solar energy facilities in the United States. Renewable Energy 92:405–414.

Watson, R. T., P. S. Kolar, M. Ferrer, T. Nygård, N. Johnston, W. G. Hunt, H. A. Smit-Robinson, C. Farmer, M. Huso, and T. Katzner. 2018. Raptor interactions with wind energy: case studies from around the world. Journal of Raptor Research 52:1–18.

Webster, M. S., P. P. Marra, S. M. Haig, S. Bensch, and R. T. Holmes. 2002. Links between worlds: unraveling migratory connectivity. Trends in Ecology and Evolution 17:76–83.

White, G. C. 2000. Population viability analysis: data requirements and essential analyses. Pages 288–331 in M. C. Pearl, L. Boitani, and T. K. Fuller, editors. Research techniques in animal ecology: controversies and consequences. Columbia University Press, New York, New York, USA.

White, G. C., and K. P. Burnham. 1999. Program MARK: survival estimation from populations of marked animals. Bird Study 46:120–138.

Williams, B. K., J. D. Nichols, and M. J. Conroy. 2002. Analysis and management of animal populations: modeling, estimation, and decision making. Academic Press, San Diego, California, USA.

Winder, V. L., A. J. Gregory, L. B. McNew, and B. K. Sandercock. 2015. Responses of male Greater Prairie-Chickens to wind energy development. Condor 117:284–296.

Zimmerman, G. S., B. A. Millsap, M. L. Avery, J. R. Sauer, M. C. Runge, and K. D. Richkus. 2019. Allowable take of black vultures in the eastern United States. Journal of Wildlife Management 83:272–282.

Zipkin, E. F., and S. P. Saunders. 2018. Synthesizing multiple data types for biological conservation using integrated population models. Biological Conservation 217:240–250.

SUPPORTING INFORMATION

Additional Supporting Information may be found online at: http://onlinelibrary.wiley.com/doi/10.1002/ecs2.3046/full

Ecosphere

Assessing population-level consequences of anthropogenic stressors for terrestrial wildlife

Todd E. Katzner[1*], Melissa A. Braham[2], Tara J. Conkling[1], Jay E. Diffendorfer[3], Adam E.

Duerr[4], Scott R. Loss[5], David M. Nelson[6], Hannah B. Vander Zanden[7], Julie L. Yee[8]

[1] *U.S. Geological Survey, Forest and Rangeland Ecosystem Science Center, Boise, ID, USA*

[2] *Division of Geology and Geography, West Virginia University, Morgantown, WV, USA*

[3] *U.S. Geological Survey, Geosciences and Environmental Change Science Center, Denver,*

Colorado, USA

[4] *Bloom Research Inc., Los Angeles, California, USA*

[5] *Department of Natural Resource Ecology & Management, Oklahoma State University,*

Stillwater, OK, USA

[6] *University of Maryland Center for Environmental Science, Appalachian Laboratory,*

Frostburg, MD, USA

[7] *University of Florida, Department of Biology, Gainesville, FL, USA*

[8] *U.S. Geological Survey, Western Ecological Research Center, Santa Cruz, CA, USA*

* Correspondence: tkatzner@usgs.gov

Appendix S1. *Detailed description of the process used to interpret demographic effects to greater roadrunners affected by solar energy in the Mojave Desert.*

1. *Framing the problem.* For the purposes of this analysis, we made several assumptions about the Mojave roadrunner population. First, we assumed no temporal variation in the location of the catchment area over the 8 years of the study and so we included all fatalities sampled in our stable isotope analysis regardless of when they occurred. Second, we assumed there was no across-year temporal variation in fatality rates. This allows us to assume that the limited monitoring data collected for these solar facilities accurately reflects actual mortality rates. Likewise, because we use data from Breeding Bird Surveys (BBS; Sauer et al. 2017) to inform population models, we assumed that the 10-year trend in BBS data incorporate fatalities at solar energy facilities within the past 5 years. See additional details in the main text.

2. *Use field-based count data to quantify the effect of the stressor on individuals.* All detail is in the main text.

3. *Characterize the location and size of the population of interest.* We used analysis of stable hydrogen isotopes in feathers from individuals killed at solar facilities, together with range maps (BirdLife International 2016) and population estimates from Partners in Flight (PIF 2019) to characterize the spatial extent and size of the population of interest. See also Fig. 2 in the main text for a flowchart describing this process.
   a. Stable hydrogen isotope analysis was performed on feather samples from 24 roadrunners killed at 3 solar facilities (Ivanpah Solar Energy Generating System, Genesis Solar Energy Center, Desert Sunlight) from 2015 to 2017 (Appendix S3: Table S1). The feather samples were cleaned using 1:200 Triton X-100 detergent, 100% ethanol, and then air-dried (Coplen and Qi, 2012). Samples were analyzed alongside international standards (USGS42; USGS43; CBS, Caribou Hoof Standard; KHS, Kudu Horn Standard; Coplen and Qi 2012; Wassenaar and Hobson 2003) and an internal keratin standard (porcine hair and skin, product # K3030; Spectrum Chemicals, New Brunswick, NJ, USA) using a comparative equilibration process (Wassenaar and Hobson, 2003) to account for exchange of keratin hydrogen with ambient vapor. Samples were analyzed for δ^2H values using a ThermoFisher high temperature conversion/elemental analyzer (TC/EA) pyrolysis unit interfaced with a ThermoFisher Delta V+ isotope ratio mass spectrometer. Values of δ^2H were normalized to the Vienna Standard Mean Ocean Water-Standard Light Antarctic Precipitation (VSMOW-SLAP) scale using USGS42, USGS43, CBS, and KHS. The δ^2H values of non-exchangeable hydrogen of these standards are -72.9, -44.4, -157.0, and -35.5‰, respectively (Wassenaar and Hobson; 2003; Soto et al. 2017).
   b. For each individual, we generated an isotope-based probability-of-origin map (Vander Zanden et al. 2018) to characterize the likelihood that the bird originated in any particular pixel within the map. We used the growing season δ^2H precipitation isoscape (Bowen et al. 2005) scaled to feather values based on the equation for a compilation of raptor feathers ($\delta^2H_{feather} = 26.59 + 1.3 * \delta^2H_{precip}$; Wunder et al. 2009) and restricted to the range map for the species (BirdLife International 2016; Fig 3). We used a pooled variance that included 1) the standard deviation of the δ^2H

precipitation isoscape calculated from the confidence intervals of the mean annual isoscape with a 20' x 20' resolution (Bowen and Revenaugh, 2003); 2) within-individual variance from the dataset itself calculated as the mean standard deviation for individuals from which more than one feather was analyzed (n = 8), which was 5.9 ‰; and 3) analytical variance, calculated as the long-term standard deviation of δ^2H values in a keratin standard at the UMCES lab, which was 2.3 ‰.

c. We then normalized this probability-of-origin map for each individual so that all pixels in a single map summed to one.

d. We averaged these 24 probability-of-origin maps and we called the averaged map an "unconstrained catchment area" (Fig. 2) because it included information about geographic origin inferred from isotope data but was not constrained by other information on roadrunner distribution and movements.

e. Then we calculated the odds ratios for each cell as (P(j)/(1-P(j))/(P(max)/(1-P(max)) (Vander Zanden et al. 2018).

f. Because the isotope data suggested that most birds were local and from a region approximately defined by the Mojave Desert Bird Conservation Region (BCR #33; Clark et al. 2000), we further modified the catchment area by constraining it to the boundaries of that BCR (Fig. 3). We focused exclusively on BCR #33 because the isotope data suggested that most of the high probability pixels were from within this BCR, suggesting that most birds grew their feathers within the BCR. The biology of the species was consistent with this, since roadrunner home ranges are small (Kelley et al. 2011, Montalvo et al. 2014), and thus even dispersing individuals likely never travel outside of the BCR. It is important to note that if the isotope data suggested that many birds originated far from the source of fatalities, we would not have focused only on BCR #33.

   The region defined by the BCR was termed a "constrained catchment area" (Fig. 2) because it includes information about geographic origin as inferred from isotope data and constrained by available ancillary information for the species. Because the boundaries of the catchment area and the BCR corresponded exactly, 100% of the BCR is within the catchment area ("proportion of BCR within the catchment area" = 1; Fig. 2, Appendix S3: Table S2).

g. Subsequently, we summed the odds ratio values for all pixels within the constrained catchment area (the "sum of pixel values in BCR" in Fig. 2 and Appendix S3: Table S2).

h. We counted the number of pixels in BCR 33 and we divided the sum of pixel values in the BCR by the total number of pixels in the BCR. We call this the "stressor-affected proportion" of the catchment area (Appendix S3: Table S2). This metric is an index that ranges from 0 to 1 and whose value is indicative of the isotope-based prediction of the likelihood that the dead birds originated from that region.

i. We obtained from the Partners in Flight Population Estimates Database (PIF 2019) the estimated number of roadrunners in BCR 33. Since there was 100% overlap between the constrained catchment area and the BCR, this estimate is the same as the area adjusted population estimate (Fig. 2; Appendix S3: Table S2; see Appendix S2 for an example where we modify the estimated population size within a BCR). For this example, we ignore the small part of the BCR within Mexico, as PIF does not provide population estimates for BCRs in Mexico.

j. We multiplied the stressor-affected proportion of the catchment area by the PIF population estimate for the BCR to estimate the proportion of the roadrunner population within the BCR that was potentially affected by fatalities at solar energy facilities.

   We call this the BCR-specific "potentially affected population" and it represents an estimate of the number of roadrunners that were potentially at risk of fatality at these five solar energy facilities in the Mojave Desert.

k. The population estimate for roadrunners in BCR 33 is 69,000 individuals and the stressor-affected proportion of the catchment area was 0.7822. Multiplying these two together suggests the potentially affected population was 53,973 birds (N_p; Tables 1, Appendix S3: Table S2).

4. *Build rate-based demographic models for the population.* We built a Bayesian integrated population model (IPM) for roadrunners in our catchment area. In brief, we developed a multi-age IPM to estimate age-specific survival and fecundity as a function of population growth and the previously-derived demographic parameters. We calculated population growth rates (λ) from BCR-specific annual indices derived from the North American Breeding Bird Survey (BBS) for 1968–2015 (Sauer et al. 2017) and we used published demographic estimates for survival ($s_a = 0.3586 \pm 0.3822$ ($\bar{x} \pm \sigma^2$); Folse and Arnold 1978, Kelley et al. 2011) and fecundity ($f = 0.88 \pm 1$, given as offspring per adult; Ohmart 1973, Hughes 2011) to inform prior distributions in the model. These reports do not provide age-specific survival estimates so we used weakly informative priors (Kruschke 2014) while constraining subadult survival to not exceed mean adult survival.

   We analyzed 3 candidate models with increasing constraints on survival and fecundity priors. This allowed us to limit non-identifiability of parameters that result from the multiple combinations of demographic parameters that produce the same estimate of λ. We then used DIC values to determine the best-fit model for subsequent analyses and we used that model as our estimate of current conditions.

   Once we identified a model of current conditions, we used survival rate estimates from the model to approximate present demography ($s_a = 0.611$, $\sigma = 0.06$). Mortality rates in these current conditions ($1 - s = 0.389$) are, implicitly, a result of all causes of death, natural and anthropogenic, and include current fatalities from solar energy generation. We multiplied the mortality rate by the estimate of population size within the catchment area to calculate the total number of individual birds within the catchment area that would be expected to die per annum (i.e., $D_t = $ total deaths per year; Table 1). Finally, we calculated the mortality rate in the absence of present levels of mortality from solar energy (s_{wos}) and we calculated the counterfactual ratio of survivorship with and without those current deaths (s_a/s_{wos}; Table 1).

5. *Assess the significance to the population of the rate changes brought on by the stressor.* We assessed the population significance of solar-caused fatalities by creating a ratio of adult survival values with and without fatalities in the Mojave Desert (Table 1). This is the Counterfactual of Impacted and Unimpacted Populations (CIU; Green et al. 2016, Cook and Robinson 2017).

   Subsequently, we performed a sensitivity analysis on the CIU to understand how uncertainty in field-based estimates of numbers of fatalities may influence our interpretation of population-level effects (Appendix S3: Table S3). To do this, we then calculated the

survival rate that would be expected with increased mortality from solar energy generation (s_{wim}) as follows,

$$s_{wim} = -(D_t - N_p)/ N_p \qquad (1)$$

We then increased the number of deaths from solar by increments of 100 to understand the consequence for survivorship. To hold survivorship levels at 95% of their current level would require 1500 fatalities of roadrunners per year. To hold them at 90% of their current level would require 3200 fatalities.

Literature Cited

BirdLife International and Handbook of the Birds of the World. 2016. Bird species distribution maps of the world. Version 6.0. Available at http://datazone.birdlife.org/species/requestdis.

Bowen, G. J. and J. Revenaugh. 2003. Interpolating the isotopic composition of modern meteoric precipitation. Water Resources Research 39:1299.

Bowen, G. J., L. I. Wassenaar and K. A. Hobson. 2005. Global application of stable hydrogen and oxygen isotopes to wildlife forensics. Oecologia 143:337–348.

Clark, J. R., D. Waller, J. A. Kushlan, G. T. Meyers, S. Senner, S. Yaich, G. Vandel, G. Fenwick, V. Mexainis, R. D. Sparrowe, A. Wentz and D. Pashley. 2000. North American Bird Conservation Initiative: Bird conservation region descriptions, a supplement to the North American Bird Conservation Initiative Bird Conservation Regions Map. US NABCI committee.

Cook, A. S. C. P. and R. A. Robinson. 2017. Towards a framework for quantifying the population-level consequences of anthropogenic pressures on the environment: The case of seabirds and windfarms. Journal of Environmental Management 190:113-121.

Coplen T. B. and H. P. Qi. 2012. USGS42 and USGS43: Human-hair stable hydrogen and oxygen isotopic reference materials and analytical methods for forensic science and implications for published measurement results. Forensic Science International 214:135-141.

Folse, Jr., L. J. and K. A. Arnold. 1978. Population ecology of roadrunners (*Geococcyx californianus*) in south Texas. The Southwestern Naturalist 23:1-27.

Green, R. E., R. H. W. Langston, A. McCluskie, R. Sutherland and J. D. Wilson, 2016. Lack of sound science in assessing wind farm impacts on seabirds. Journal of Applied Ecology 53:1635-1641.

Hughes, J. M. 2011. Greater Roadrunner (*Geococcyx californianus*), version 2.0. *In* Poole, A. F. editor. The Birds of North America. Cornell Lab of Ornithology, Ithaca, New York, USA.

Kelley, S. W., D. Ransom Jr., J. A. Butcher, G. G. Shulz, B. W. Surber, W. E. Pinchak, S. A. Santamaria and L. A. Hurtado. 2011. Home range dynamics, habitat selection, and survival of Greater Roadrunners. Journal of Field Ornithology 82:165-174.

Kruschke, J. 2014. Doing Bayesian data analysis: A tutorial with R, JAGS, and Stan. Academic Press, London, United Kingdom.

Montalvo, A. E., D. Ransom Jr., R. R. Lopez. 2014. Greater roadrunner (*Geococcyx californianus*) home range and habitat selection in west Texas. Western North American Naturalist 74:201-207.

Partners in Flight (PIF). 2019. Population Estimates Database, version 3.0. Available at
        http://pif.birdconservancy.org/PopEstimates. Accessed April 14, 2019.

Sauer J., D. K. Niven, J. E. Hines, D. J. Ziolowski Jr., K. L. Pardieck, J. E. Fallon, and W. L.
        Link. 2017. The North American Breeding Bird Survey, Results and Analysis 1966 -
        2015. Version 2.07.2017 USGS Patuxent Wildlife Research Center, Laurel, Maryland.

Soto, D. X., G. Koehler, L. I. Wassenaar, and K. A. Hobson. 2017. Re-evaluation of the
        hydrogen stable isotopic composition of keratin calibration standards for wildlife and
        forensic science applications. Rapid Communications in Mass Spectrometry 31:1193-
        1203.

Ohmart, R. D. 1973. Observations on the breeding adaptations of the roadrunner. The Condor
        75:140-149.

Vander Zanden, H., D. Nelson, M. Wunder, T. Conkling and T. Katzner. 2018. Application of
        isoscapes to determine geographic origin of terrestrial wildlife for conservation and
        management. Biological Conservation 228:268–280.

Wassenaar L. I. and K. A. Hobson. 2003. Comparative equilibration and online technique for
        determination of non-exchangeable hydrogen of keratins for use in animal migration
        studies. Isotopes in Environmental and Health Studies 39:211-217.

Wunder, M. B., K. A. Hobson, J. Kelly, P. P. Marra, L. I. Wassenaar, C. A. Stricker, and R. R.
        Doucett. 2009. Does a Lack of Design and Repeatability Compromise Scientific
        Criticism? A Response to Smith et al. The Auk 126:922–926.

Ecosphere

Assessing population-level consequences of anthropogenic stressors for terrestrial wildlife

Todd E. Katzner[1*], Melissa A. Braham[2], Tara J. Conkling[1], Jay E. Diffendorfer[3], Adam E.

Duerr[4], Scott R. Loss[5], David M. Nelson[6], Hannah B. Vander Zanden[7], Julie L. Yee[8]

[1] *U.S. Geological Survey, Forest and Rangeland Ecosystem Science Center, Boise, ID, USA*

[2] *Division of Geology and Geography, West Virginia University, Morgantown, WV, USA*

[3] *U.S. Geological Survey, Geosciences and Environmental Change Science Center, Denver,*

Colorado, USA

[4] *Bloom Research Inc., Los Angeles, California, USA*

[5] *Department of Natural Resource Ecology & Management, Oklahoma State University,*

Stillwater, OK, USA

[6] *University of Maryland Center for Environmental Science, Appalachian Laboratory,*

Frostburg, MD, USA

[7] *University of Florida, Department of Biology, Gainesville, FL, USA*

[8] *U.S. Geological Survey, Western Ecological Research Center, Santa Cruz, CA, USA*

* Correspondence: tkatzner@usgs.gov

Appendix S2. *Detailed description of the process used to interpret demographic effects to red-tailed hawks affected by wind turbines at Altamont Pass Wind Resource Area.*

1. *Framing the problem.* We made similar assumptions here as in the roadrunner example. First, we again used BBS data in our models (Sauer et al. 2017) and we included all sampled fatalities in our stable isotope analysis regardless of the date on which the carcass was found. Second, field fatality data and dead birds were available for the time period 2005 – 2017 and thus interpretation of our analyses is appropriate for that time period. However, the time frame for the collection of fatality data (2007 – 2017) does not match exactly with the time frame in which tissue samples were collected from carcasses. For simplicity, we assume that this difference is unimportant to our results. See additional details in the main text.

2. *Use field-based count data to quantify the effect of the stressor on individuals.* All detail is in the main text.

3. *Characterize the location and size of the population of interest.* We again used analysis of stable hydrogen isotopes in feathers from individuals killed at APWRA, together with range maps, flyway maps and population estimates from Partners in Flight (PIF 2019) to characterize the population of interest. See also Fig. 2 in the main text for a flowchart describing this process.
    a. Stable isotope analysis was performed as in Appendix S1 and relied on feather samples from 86 red-tailed hawks killed at APWRA during 2007 – 2017 (Appendix S3: Table S4).
    b. For each individual, we generated an isotope-based probability of origin map as in step 3b of Appendix S1. Again, we used the raptor feather equation to rescale the growing season precipitation isoscape and constrained to the red-tailed hawk range map (BirdLife International 2016; Fig 4). The pooled variance process was the same, except the individual variance measured in red-tailed hawks was 5.6 ‰ (n=9).
    c. We used geographic assignment process with a 5:1 odds ratio threshold to characterize individual hawks as "local" or "non-local" (i.e., recent migrants or itinerants) to the region around APWRA (this odds-ratio assignment process is described in detail in Vander Zanden et al. 2018). We classified 33 birds as local and 53 as non-local.
    d. We then normalized the probability of origin maps so that all pixels summed to 1 in each map, averaged them separately across local and non-local birds, and calculated the odds ratios for each cell in the two maps, to form "unconstrained catchment areas" as detailed in Appendix S1, 3c, d and e.
    e. We restricted the two maps (local and non-local) resulting from (d) to the area defined by a 5:1 odds ratio (Fig. 2, Fig. 4). At this point, the analyses diverged slightly for the local and non-local populations. Steps f through j address the non-local populations, whereas step k addresses the local populations.
    f. We further restricted the non-local area to a range defined by flyways. Because red-tailed hawks from California are known to cross between the Pacific and Central Flyways (USFWS 2015, Bloom et al. 2015), we retained all pixels from these two flyways. However, we did not expect these birds to enter into the Mississippi and Atlantic Flyways, so we excluded those pixels. We called the resulting map a

"constrained catchment area".

g. We overlaid North American Bird Conservation Regions (BCRs, Fig. 4; Clark et al. 2000) on the two constrained catchment areas. We excluded portions of the constrained catchment area that overlapped BCRs in Mexico, as PIF does not provide population estimates for those BCRs.

h. For the non-local constrained catchment area, within each BCR that overlapped any part of the catchment area, we calculated the percentage of the area of the BCR that overlapped the catchment area. We called this the "proportion of BCR within the catchment area" (Fig. 2, Appendix S3: Table S5). For each BCR, we then calculated the # of cells in the catchment area, the sum of pixel values, and the stressor-affected proportion of the population (Appendix S3: Table S5), as in the prior example.

i. For each BCR in the non-local catchment area, we again obtained the estimated population size of red-tailed hawks from the Partners in Flight Population Estimates Database (PIF 2019). We multiplied that number by the proportion of the BCR within the catchment area to estimate the number of birds from that BCR in the catchment area (Appendix S3: Table S5). In cases where the BCR boundary overlapped the boundary of the Central Flyway, we used the PIF estimated population size for the full BCR, rather than adjusting that PIF estimate by the proportion of the BCR within in the Central Flyway. We call this the "area adjusted population estimate" for the BCR. This approach assumes an even distribution of birds across the BCR. Although imperfect, we use this approach because it allows us to account for the fact that the boundaries of the BCR do not line up perfectly with those of the catchment area.

j. For each BCR in the non-local catchment area, we then multiplied the stressor-affected proportion of the catchment area (as defined in Appendix S1, step 3h) by the area adjusted population estimate to estimate the potentially affected population (Appendix S3: Table S5). In this case, this metric incorporates information about both the proportion of the BCR that falls within the catchment area and the likelihood of origin of feathers from that BCR (in the roadrunner example, the metric only incorporated likelihood of origin information, because we did not have to account for partial overlap of BCRs and the catchment area).

k. The boundary of the odds ratio-defined area describing the local catchment area followed the majority of the boundary of BCR #32, the BCR in which APWRA is located. We therefore assumed that the catchment area for these birds was defined by the BCR. We then followed steps g to step j, above, to calculate a potentially affected population of red-tailed hawks in BCR #32 (Appendix S3: Table S5). This process was very similar to the process implemented in the roadrunner example.

l. Subsequently, we summed the potentially affected populations for all local and non-local BCRs. This process resulted in estimates of 98,217 and 605,484 red-tailed hawks within the local and non-local potentially affected populations, respectively (N_p; Tables 1, Appendix S3: Table S5). Thus, in total we estimate that there are 703,755 total birds potentially affected by this stressor.

4. *Build demographic models for the population.* We again built a Bayesian integrated population model (IPM) for red-tailed hawks in each of the two potentially affected populations (local and non-local). These models were constructed as before and again based on BBS data (Sauer et al. 2017). We used demographic estimates for juvenile ($s_j = 0.4075 \pm$

0.0427 ($\bar{x} \pm \sigma^2$); Henny and Wight 1972, Luttich et al. 1971) and adult survival ($s_a = 0.7750 \pm 0.0004$; Henny and Wight 1972) and fecundity ($f = 0.7079 \pm 1.031$, given as offspring per adult; derived from 14 citations given in Preston and Beane 2009) found in existing literature to inform prior distributions in the model. We analyzed candidate models and information theoretic data as before to estimate current conditions.

We again used survivorship rates estimated from the best fit model to approximate current conditions ($s_a = 0.795$, $\sigma = 0.02$; here we ignore juvenile survival and we assume that adult survival is the same for local and non-local birds). We assumed all fatalities were adults and we used mortality rates to estimate D_t for red-tailed hawks in each BCR, in the local and non-local populations, and in the combined potentially affected population (Table 1).

Our stable isotope data suggested that 38% of birds killed each year are local. Thus, of the 169 deaths per year, 64 are local and 105 are non-local (Table 1). From this we were able to estimate s_{wos} and the CIU as in the prior example, but this time for both the local and non-local catchment areas (Tables 1, Appendix S3: Table S6).

5. *Assess the significance to the population of the rate changes brought on by the stressor.* Finally, we assessed the significance to the population of the impact of fatalities caused by wind energy with the CIU and a sensitivity analysis on this metric, as before (Table 1, Appendix S3: Table S6). Details of this are in the main text.

Literature Cited

BirdLife International and Handbook of the Birds of the World. 2016. Bird species distribution maps of the world. Version 6.0. Available at http://datazone.birdlife.org/species/requestdis.

Bloom, P. H., M. D. McCreary, J. M. Scott, J. M. Papp, K. J. Sernka, S. E. Thomas, J. W. Kidd, E. H. Henkel, J. L. Henkel and M. J. Gibson. 2015. Northward summer migration of red-tailed hawks fledged from southern latitudes. Journal of Raptor Research 49:1-17

Bowen, G. J. and J. Revenaugh. 2003. Interpolating the isotopic composition of modern meteoric precipitation. Water Resources Research 39:1299.

Bowen, G. J., L. I. Wassenaar and K. A. Hobson. 2005. Global application of stable hydrogen and oxygen isotopes to wildlife forensics. Oecologia 143:337–348.

Clark, J. R., D. Waller, J. A. Kushlan, G. T. Meyers, S. Senner, S. Yaich, G. Vandel, G. Fenwick, V. Mexainis, R. D. Sparrowe, A. Wentz and D. Pashley. 2000. North American Bird Conservation Initiative: Bird conservation region descriptions, a supplement to the North American Bird Conservation Initiative Bird Conservation Regions Map. US NABCI committee.

Coplen T. B. and H. P. Qi. 2012. USGS42 and USGS43: Human-hair stable hydrogen and oxygen isotopic reference materials and analytical methods for forensic science and implications for published measurement results. Forensic Science International 214:135-141.

Henny, C. J. and H. M. Wight. 1972. Population ecology and environmental pollution: red-tailed hawk and Cooper's hawk. US FWS Wildlife Research Report 2:229-250.

Luttich, S. N., L. B. Keith and J. D. Stephenson. 1971. Population dynamics of the red-tailed hawk (*Buteo jamaicensis*) at Rochester, Alberta. The Auk 88:75-87.

Partners in Flight (PIF). 2019. Population Estimates Database, version 3.0. Available at http://pif.birdconservancy.org/PopEstimates. Accessed April 14, 2019.

Preston, C. R. and R. D. Beane. 2009. Red-tailed Hawk (*Buteo jamaicensis*), version 2.0. *In* Poole, A. F. editor. The Birds of North America. Cornell Lab of Ornithology, Ithaca, New York, USA.

Sauer J., D. K. Niven, J. E. Hines, D. J. Ziolowski Jr., K. L. Pardieck, J. E. Fallon, and W. L. Link. 2017. The North American Breeding Bird Survey, Results and Analysis 1966 - 2015. Version 2.07.2017 USGS Patuxent Wildlife Research Center, Laurel, Maryland.

USFWS. 2015. USFWS Administrative Waterfowl Flyway Boundaries. Available at: https://ecos.fws.gov/ServCat/Reference/Profile/42276

Vander Zanden, H., D. Nelson, M. Wunder, T. Conkling and T. Katzner. 2018. Application of isoscapes to determine geographic origin of terrestrial wildlife for conservation and management. Biological Conservation 228:268–280.

Wassenaar L. I. and K. A. Hobson. 2003. Comparative equilibration and online technique for determination of non-exchangeable hydrogen of keratins for use in animal migration studies. Isotopes in Environmental and Health Studies 39:211-217.

Wunder, M. B., K. A. Hobson, J. Kelly, P. P. Marra, L. I. Wassenaar, C. A. Stricker, and R. R. Doucett. 2009. Does a Lack of Design and Repeatability Compromise Scientific Criticism? A Response to Smith et al. The Auk 126:922–926.

Ecosphere

Assessing population-level consequences of anthropogenic stressors for terrestrial wildlife

Todd E. Katzner[1][*], Melissa A. Braham[2], Tara J. Conkling[1], Jay E. Diffendorfer[3], Adam E. Duerr[4], Scott R. Loss[5], David M. Nelson[6], Hannah B. Vander Zanden[7], Julie L. Yee[8]

[1] *U.S. Geological Survey, Forest and Rangeland Ecosystem Science Center, Boise, ID, USA*

[2] *Division of Geology and Geography, West Virginia University, Morgantown, WV, USA*

[3] *U.S. Geological Survey, Geosciences and Environmental Change Science Center, Denver, Colorado, USA*

[4] *Bloom Research Inc., Los Angeles, California, USA*

[5] *Department of Natural Resource Ecology & Management, Oklahoma State University, Stillwater, OK, USA*

[6] *University of Maryland Center for Environmental Science, Appalachian Laboratory, Frostburg, MD, USA*

[7] *University of Florida, Department of Biology, Gainesville, FL, USA*

[8] *U.S. Geological Survey, Western Ecological Research Center, Santa Cruz, CA, USA*

* Correspondence: tkatzner@usgs.gov

Table S1 – Stable hydrogen isotope data for feathers collected from greater roadrunners (GRRO) killed at solar facilities in the Mojave Desert. Data provided are the mean δ^2H of the 1-3 feathers analyzed per bird. See main text and Appendix S1 for details on origin of birds and how these data were used.

Individual	Species	Mean δ^2H
1	GRRO	-38.346
2	GRRO	-15.86
3	GRRO	-11.882
4	GRRO	-16.492
5	GRRO	-1.738
6	GRRO	-3.04
7	GRRO	-8.146
8	GRRO	-25.24
9	GRRO	-17.32
10	GRRO	-7.57
11	GRRO	-7.5
12	GRRO	-26.57
13	GRRO	-34.18
14	GRRO	-13.6
15	GRRO	-33.18
16	GRRO	-27.43
17	GRRO	-30.54
18	GRRO	-32.56
19	GRRO	-28.36
20	GRRO	-26.7
21	GRRO	-27.48
22	GRRO	-29.11
23	GRRO	-27.15
24	GRRO	6.47

Table S2 – Calculations applied to each Bird Conservation Region (BCR, Clark et al. 2000) to estimate the number of greater roadrunners from each BCR that are at risk from an anthropogenic stressor (solar energy). The catchment area was defined based on the borders of BCR #33, thus in this example all pixels in the BCR were also within the catchment area (that is not the case in the subsequent example). The "sum of pixels in the catchment area" is the sum of the odds ratio values, estimated from hydrogen isotope derived probability of origin maps, for all pixels within the constrained catchment area. Maximum value of all cells within the probability of origin map was normalized to 1. PIF population estimates for the BCR are from PIF (2019). Mexico was excluded because PIF population estimates are not available for the area.

BCR #	Pixels out of catchment area	Pixels in catchment area	Proportion of BCR within catchment area	Sum of values of pixels in catchment area	Stressor affected proportion of BCR[a]	PIF population estimate for BCR	Area adjusted population estimate for BCR[b]	Number of birds at risk in constrained catchment area[c]	Number of birds in potentially affected population N_p
33	0	199	1	155.66	0.78	69,000	69,000	53,973	53,973

[a] Stressor affected proportion of the BCR = (sum of values of pixels in catchment area)/(pixels in catchment area).
[b] Area adjusted population estimate for the BCR = (PIF population estimate for BCR)*(proportion of BCR within catchment area)
[c] Number of birds at risk in the constrained catchment area = (area adjusted population estimate for the BCR)*(stressor affected proportion of BCR)

Table S3 - Sensitivity analysis illustrating potential consequences of anthropogenic stressors on terrestrial wildlife. Shown below is an analysis of the result of variation in numbers of greater roadrunners killed at solar energy facilities in the Mojave Desert, California, USA on changes to a counterfactual ratio (CIU; calculation described in main text). D_s is deaths from the stressor (solar energy). D_t is total number of deaths per annum, calculated initially by multiplying current survival (0.611 in this case) by N_p (number of animals potentially at risk from the stressor; 53,973 in this case) and subsequently by adding additional deaths from the stressor (D_s). See main text and Appendix S1 for details on the calculations applied and the source of original parameter values. Rows highlighted in yellow are discussed in the text.

D_s	D_t	Survival with increased mortality	CIU	D_s	D_t	Survival with increased mortality	CIU
64	20,996	0.611	1.000	2400	23,396	0.567	0.927
100	21,096	0.609	0.997	2500	23,496	0.565	0.924
200	21,196	0.607	0.994	2600	23,596	0.563	0.921
300	21,296	0.605	0.991	2700	23,696	0.561	0.918
400	21,396	0.604	0.988	2800	23,796	0.559	0.915
500	21,496	0.602	0.985	2900	23,896	0.557	0.912
600	21,596	0.600	0.982	3000	23,996	0.555	0.909
700	21,696	0.598	0.979	3100	24,096	0.554	0.906
800	21,796	0.596	0.976	3200	24,196	0.552	0.903
900	21,896	0.594	0.973	3300	24,296	0.550	0.900
1000	21,996	0.592	0.970	3400	24,396	0.548	0.897
1050	22,046	0.592	0.968	3500	24,496	0.546	0.894
1060	22,056	0.591	0.968	3600	24,596	0.544	0.891
1070	22,066	0.591	0.968	3700	24,696	0.542	0.888
1080	22,076	0.591	0.967	3800	24,796	0.541	0.885
1100	22,096	0.591	0.967	3900	24,896	0.539	0.882
1200	22,196	0.589	0.964	4000	24,996	0.537	0.879
1300	22,296	0.587	0.961	4100	25,096	0.535	0.876
1400	22,396	0.585	0.958	4200	25,196	0.533	0.873
1500	22,496	0.583	0.955	4300	25,296	0.531	0.870
1600	22,596	0.581	0.951	4400	25,396	0.529	0.867
1700	22,696	0.580	0.948	4500	25,496	0.528	0.864
1800	22,796	0.578	0.945	4600	25,596	0.526	0.861
1900	22,896	0.576	0.942	4700	25,696	0.524	0.857
2000	22,996	0.574	0.939	4800	25,796	0.522	0.854
2100	23,096	0.572	0.936	4900	25,896	0.520	0.851
2200	23,196	0.570	0.933	5000	25,996	0.518	0.848
2270	23,266	0.569	0.931				
2280	23,276	0.569	0.931				
2300	23,296	0.568	0.930				

Table S4 – Mean stable hydrogen isotope data for feathers collected from red-tailed hawks (RTHA) killed at Altamont Pass Wind Resource Area. Data provided are the mean δ^2H of the 1-3 feathers analyzed per bird. See main text and Appendix S2 for details on origin of birds and how these data were used.

Individual	Species	Mean δ^2H	Individual	Species	Mean δ^2H	Individual	Species	Mean δ^2H
1	RTHA	-50.4445				64	RTHA	-23.11
2	RTHA	-34.702	33	RTHA	-28.43	65	RTHA	-54.31
3	RTHA	-24.8509	34	RTHA	-61.56	66	RTHA	-22.31
4	RTHA	-51.11	35	RTHA	-32.06	67	RTHA	-43.22
5	RTHA	-42.87	36	RTHA	-20.37	68	RTHA	-44.36
6	RTHA	-24.24	37	RTHA	-5.67	69	RTHA	-59
7	RTHA	-25.21	38	RTHA	-15.21	70	RTHA	-48.94
8	RTHA	-27.12	39	RTHA	-37.89	71	RTHA	-59.45
9	RTHA	-20.42	40	RTHA	-52.28	72	RTHA	-77.89
10	RTHA	-70.41	41	RTHA	-59.23	73	RTHA	-19.25
11	RTHA	-21.96	42	RTHA	-56.71	74	RTHA	-17.07
12	RTHA	-88.04	43	RTHA	-53.03	75	RTHA	16.57
13	RTHA	-44.91	44	RTHA	-61.32	76	RTHA	-38.43
14	RTHA	-72.75	45	RTHA	-62.17	77	RTHA	-30.48
15	RTHA	-65.69	46	RTHA	-23.67	78	RTHA	-51.2433
16	RTHA	-21.9	47	RTHA	-34.32	79	RTHA	-60.0667
17	RTHA	-19.43	48	RTHA	-25.4	80	RTHA	-19.2467
18	RTHA	-43.96	49	RTHA	-29.97	81	RTHA	-43.3167
19	RTHA	-60.86	50	RTHA	-79.47	82	RTHA	-18.3467
20	RTHA	-22.84	51	RTHA	-27.09	83	RTHA	-51.49
21	RTHA	-26.37	52	RTHA	-10.18	84	RTHA	-83.45
22	RTHA	-20.57	53	RTHA	-35.03	85	RTHA	-39.74
23	RTHA	-46.04	54	RTHA	-29.12	86	RTHA	-54.13
24	RTHA	-73.38	55	RTHA	-6.26			
25	RTHA	-33.68	56	RTHA	-39.6			
26	RTHA	-45.25	57	RTHA	-46.77			
27	RTHA	-24.96	58	RTHA	-52.09			
28	RTHA	-27.73	59	RTHA	-46.66			
29	RTHA	-35.87	60	RTHA	-80.09			
30	RTHA	-34.17	61	RTHA	-66.35			
31	RTHA	-22.22	62	RTHA	-38.39			
32	RTHA	-41.02	63	RTHA	-27.52			

Table S5 – Calculations applied to each Bird Conservation Region (BCR, Clark et al. 2000) to estimate the number of red-tailed hawks from each BCR that are at risk from an anthropogenic stressor (wind turbines). The catchment area was defined based on an odds ratio approach as defined in the main text and Appendix S2. The "sum of pixels in the catchment area" is the sum of the odds ratio values, estimated from hydrogen isotope derived probability of origin maps, for all pixels within the constrained catchment area. Maximum value of all cells within the probability of origin map was normalized to 1. PIF population estimates for the BCR are from PIF (2019). Mexico was excluded because PIF population estimates are not available for the area.

BCR #	Pixels out of catchment area	Pixels in catchment area	Proportion of BCR within catchment area	Sum of values of pixels in catchment area	Stressor affected proportion of BCR[a]	PIF population estimate for BCR	Area adjusted population estimate for BCR[b]	Number of birds at risk in constrained catchment area[c]	Number of birds in potentially affected population N_p[d]
Non-local red-tailed hawks									
5	263	230	0.467	131.776	0.573	52,000	24,260	13,899	605,484
9	19	736	0.975	440.819	0.599	340,000	331,444	198,514	
10	639	409	0.390	147.172	0.360	190,000	74,151	26,682	
11	565	234	0.293	110.728	0.473	370,000	108,360	51,276	
15	0	48	1.000	36.543	0.761	7,900	7,900	6,014	
16	0	473	1.000	346.727	0.733	110,000	110,000	80,634	
17	105	274	0.723	88.149	0.322	91,000	65,789	21,165	
18	58	296	0.836	172.110	0.581	92,000	76,927	44,729	
19	163	206	0.558	120.322	0.584	190,000	106,070	61,954	
22	42	59	0.584	25.107	0.426	160,000	93,465	39,773	
32	109	29	0.210	12.343	0.426	150,000	31,522	13,416	
33	145	65	0.310	33.934	0.522	79,000	24,452	12,766	
34	4	103	0.963	59.384	0.577	36,000	34,654	19,980	
35	58	105	0.644	43.512	0.414	55,000	35,429	14,682	
Local red-tailed hawks									
32	0	138	1.000	90.359	0.655	150,000	150,000	98,217	98,217

[a] Stressor affected proportion of the BCR = (sum of values of pixels in catchment area)/(pixels in catchment area).
[b] Area adjusted population estimate for the BCR = (PIF population estimate for BCR)*(proportion of BCR within catchment area)
[c] Number of birds at risk in the constrained catchment area = (area adjusted population estimate for the BCR)*(stressor affected proportion of BCR)
[d] N_p is the sum of the number of birds at risk in each BCR (i.e., the sum of the prior column).

Table S6 - Sensitivity analysis illustrating potential consequences of anthropogenic stressors on terrestrial wildlife. Shown below is an analysis of the result of variation in numbers of red-tailed hawks killed at Altamont Pass Wind Resource Area on changes to a counterfactual ratio (CIU; calculation described in main text). Two analyses were conducted, one for local populations and the other for non-local populations; see main text for details on these designations. D_s is deaths from the stressor (wind energy). D_t is total number of deaths per annum, calculated initially by multiplying current survival (0.795 in this case) by N_p (number of animals potentially at risk from the stressor; 605,484 in the non-local catchment area and 98,217 in the local catchment area) and subsequently by adding additional deaths from the stressor (D_s). See main text and Appendix S1 for details on the calculations applied and the source of original parameter values. Rows highlighted in yellow are discussed in the text.

A. Non-local red-tailed hawks

D_s	D_t	Survival with increased mortality	CIU	D_s	D_t	Survival with increased mortality	CIU
105	124,124	0.795	1.000	2600	126,724	0.791	0.995
100	124,224	0.795	1.000	2700	126,824	0.791	0.994
200	124,324	0.795	1.000	2800	126,924	0.790	0.994
300	124,424	0.795	0.999	2900	127,024	0.790	0.994
400	124,524	0.794	0.999	3000	127,124	0.790	0.994
500	124,624	0.794	0.999	3100	127,224	0.790	0.994
600	124,724	0.794	0.999	3200	127,324	0.790	0.993
700	124,824	0.794	0.999	3300	127,424	0.790	0.993
800	124,924	0.794	0.998	3400	127,524	0.789	0.993
900	125,024	0.794	0.998	3500	127,624	0.789	0.993
1000	125,124	0.793	0.998	3600	127,724	0.789	0.993
1100	125,224	0.793	0.998	3700	127,824	0.789	0.992
1200	125,324	0.793	0.998	3800	127,924	0.789	0.992
1300	125,424	0.793	0.997	3900	128,024	0.789	0.992
1400	125,524	0.793	0.997	4000	128,124	0.788	0.992
1500	125,624	0.793	0.997	4100	128,224	0.788	0.991
1600	125,724	0.792	0.997	4200	128,324	0.788	0.991
1700	125,824	0.792	0.996	4300	128,424	0.788	0.991
1800	125,924	0.792	0.996	4400	128,524	0.788	0.991
1900	126,024	0.792	0.996	4500	128,624	0.788	0.991
2000	126,124	0.792	0.996	4600	128,724	0.787	0.990
2100	126,224	0.792	0.996	4700	128,824	0.787	0.990
2200	126,324	0.791	0.995	4800	128,924	0.787	0.990
2300	126,424	0.791	0.995	4900	129,024	0.787	0.990
2400	126,524	0.791	0.995	5000	129,124	0.787	0.990
2500	126,624	0.791	0.995				

B. Local red-tailed hawks

D_s	D_t	Survival with increased mortality	CIU	D_s	D_t	Survival with increased mortality	CIU
64	20,134	0.795	1.000	2600	22,734	0.769	0.967
100	20,234	0.794	0.999	2700	22,834	0.768	0.965
200	20,334	0.793	0.997	2800	22,934	0.766	0.964
300	20,434	0.792	0.996	2900	23,034	0.765	0.963
400	20,534	0.791	0.995	3000	23,134	0.764	0.962
500	20,634	0.790	0.994	3100	23,234	0.763	0.960
600	20,734	0.789	0.992	3200	23,334	0.762	0.959
700	20,834	0.788	0.991	3300	23,434	0.761	0.958
800	20,934	0.787	0.990	3400	23,534	0.760	0.956
900	21,034	0.786	0.988	3500	23,634	0.759	0.955
1000	21,134	0.785	0.987	3600	23,734	0.758	0.954
1100	21,234	0.784	0.986	3700	23,834	0.757	0.953
1200	21,334	0.783	0.985	3800	23,934	0.756	0.951
1300	21,434	0.782	0.983	3900	24,034	0.755	0.950
1400	21,534	0.781	0.982	4000	24,134	0.754	0.949
1500	21,634	0.780	0.981	4100	24,234	0.753	0.947
1600	21,734	0.779	0.980	4200	24,334	0.752	0.946
1700	21,834	0.778	0.978	4300	24,434	0.751	0.945
1800	21,934	0.777	0.977	4400	24,534	0.750	0.944
1900	22,034	0.776	0.976	4500	24,634	0.749	0.942
2000	22,134	0.775	0.974	4600	24,734	0.748	0.941
2100	22,234	0.774	0.973	4700	24,834	0.747	0.940
2200	22,334	0.773	0.972	4800	24,934	0.746	0.939
2300	22,434	0.772	0.971	4900	25,034	0.745	0.937
2400	22,534	0.771	0.969	5000	25,134	0.744	0.936
2500	22,634	0.770	0.968				

Literature Cited

Clark, J. R., D. Waller, J. A. Kushlan, G. T. Meyers, S. Senner, S. Yaich, G. Vandel, G.
        Fenwick, V. Mexainis, R. D. Sparrowe, A. Wentz and D. Pashley. 2000. North American
        Bird Conservation Initiative: Bird conservation region descriptions, a supplement to the
        North American Bird Conservation Initiative Bird Conservation Regions Map. US
        NABCI committee.
Partners in Flight (PIF). 2019. Population Estimates Database, version 3.0. Available at
        http://pif.birdconservancy.org/PopEstimates. Accessed 14 April 2019.